

1-1-2017

# Fam129b, A Novel Adherent Junction Protein, Forms A Complex With Keap1

Fatme Ali Hachem  
*Wayne State University,*

Follow this and additional works at: [https://digitalcommons.wayne.edu/oa\\_theses](https://digitalcommons.wayne.edu/oa_theses)



Part of the [Biochemistry Commons](#)

---

## Recommended Citation

Hachem, Fatme Ali, "Fam129b, A Novel Adherent Junction Protein, Forms A Complex With Keap1" (2017). *Wayne State University Theses*. 564.

[https://digitalcommons.wayne.edu/oa\\_theses/564](https://digitalcommons.wayne.edu/oa_theses/564)

This Open Access Thesis is brought to you for free and open access by DigitalCommons@WayneState. It has been accepted for inclusion in Wayne State University Theses by an authorized administrator of DigitalCommons@WayneState.

**FAM129B, A NOVEL ADHERENT JUNCTION PROTEIN, FORMS A COMPLEX WITH  
KEAP1**

by

**FATME HACHEM**

**THESIS**

Submitted to the Graduate School

of Wayne State University,

Detroit, Michigan

in partial fulfillment of the requirements

for the degree of

**MASTER OF SCIENCE**

2017

MAJOR:

**BIOCHEMISTRY AND  
MOLECULAR BIOLOGY**

Approved by:

---

Advisor

Date

## **DEDICATION**

I would like to dedicate this thesis to My husband, Yue Ren, for his ongoing support encouragement, and helping me when I needed help the most . I also thank my parents for their unconditional faith in me.

## **ACKNOWLEDGMENTS**

My earnest and eternal gratitude is to my advisor, Dr. David Evans. He has mentored me through my work, and has helped me become a better person. I would also like to express thanks and gratitude to my graduate committee, Dr. Brian Edwards and Dr. Mostapaha Kandouz.

Finally, I am thankful to my labmates: Chandni Patel, Lakshmi, and Dr. Song Chen. I am also grateful and thankful to Asmita Vaishnav for helping start out in the lab.

## TABLE OF CONTENTS

Dedication	ii
Acknowledgements	iii
Table of Contents	iii
List of Figures	vii
Chapter 1 : Introduction	1
1.1 FAM129B	1
1.2 Domain Structure of FAM129B	2
1.3 Apoptosis	4
1.4 Cancer Cell and Metastasis	7
Chapter 2: Materials and Methods	11
2.1 Vectors Used in This Study	11
2.1 PCR and Cloning	11
2.3 Agarose Gel Electrophoreses	12
2.4 Cell Culture	12
2.5 Freezing and Thawing Cell Culture	14
2.6 Soluble Protein Fraction	14
2.7 SDS-PAGE	14
2.8 Western Blotting	15
2.9 Co-Immunoprecipitations	16

2.10 Protein Expression in <i>E.coli</i>	16
2.11 Bacterial Cell Lysis	17
2.12 Recombinant Protein Purification	18
2.13 Buffer Exchange and Protein Concentrating	18
2.14 GST Pull Down Assay	19
Chapter 3: Structural Characterization of FAM129B	20
3.1 Introduction	20
3.2 Material and Methods	21
3.3 Results	25
3.4 Discussion	29
Chapter 4: Characterization of the Interaction between FAM129B and KEAP1	33
4.1 Introduction	33
4.2 Material and Methods	37
4.3 Results	40
4.4 Discussion	48
Chapter 5: The Role of FAM129B in Cancer Cell Invasion	50
5.1 Introduction	50
5.2 Material and Methods	52
5.3 Results	53
5.4 Discussion	60

References	63
Abstract	68
Autobiographical Statement	70

## LIST OF FIGURES

Figure 1.1 Domain Structure of FAM129B.....	3
Figure 1.2 Intrinsic apoptotic Pathway.....	4
Figure 1.3 The Fas-mediated apoptotic pathway .....	5
Figure 1.4 The TNF $\alpha$ Apoptotic Pathway.....	7
Figure 3.1 Purification of His-FAM129B.....	25
Figure 3.2 FAM129B exist as a dimer.....	26
Figure 3,3 Circular Dichroism Analysis of FAM129B.....	27
Figure 3.4. Crystallization Screening Results of Purified FAM129B .....	28
Figure 3.5. Disorder Predication Analysis.....	31
Figure 3.6. Seleno-Methionine labelled FAM129B Protein Purification gel.....	32
Figure 4.1. Domain Structure of KELCH-Like Associated Protein 1 (KEAP1).....	34
Figure 4.2. Working Model of Hypothesis.....	36
Figure 4.3. PCR results for the amplification of KEAP1 and the corresponding Deletion Constructs. ....	41
Figure 4.4 Purification of GST tagged KEAP1, GST-KELCH, and GST-KEAP1 $\Delta$ KELCH.....	43



Figure 4.5. FAM129B interacts with KEAP1 through its ETGE motif.....	45
Figure 4.6 FAM129B interacts with KEAP1 directly through the KECLH repeats of KEAP1.....	46
Figure 4.7 FAM129B and KEAP1 seem to co-localize upon TNF $\alpha$ treatment in HeLa Cells.....	47
Figure 5.1. FAM129B co-localizes with N-Cadherin in Confluent HeLa cells.....	54
Figure 5.2. Knockdown of N-Cadherin expression in HeLa seems to inhibit FAM129B localization to the membrane.....	55
Figure 5.3. FAM129B is phosphorylated by MAP Kinase.....	57
Figure 5.4. FAM129B phosphorylation by MAP kinase seems to translocate FAM129B to the membrane.....	58
Figure 5.5. FAM129B expression level increases when EMT is induced by TGF $\beta$ .....	59

## CHAPTER 1

### INTRODUCTION

#### 1.1 FAM129B

FAM129B, also known as MINERVA or Niban-like Protein 1, is part of a small family of proteins that includes FAM129A and FAM129C. Little is known about the structure and functions of these proteins except that all 3 proteins have been implicated in cancer. FAM129A has been reported to be expressed in different types of cancer and is shown to be involved in cancer cell proliferation[1]. FAM129C has been shown to be highly expressed in patients with chronic lymphocytic leukemia (CLL)[2]. A proteomics study in 2009 by Old et al. was the first paper to mention FAM129B. In this study FAM129B was shown to be highly expressed in melanoma cells, an invasive skin cancer cell line, and implicated in cancer cell invasion[3].

In the subsequent years after the Old et al study, FAM129B was mentioned in a modest number of publications. In 2011, a study published in our lab reported that FAM129B is associated with the adherent junctions in confluent HeLa cells and suppressed the TNF $\alpha$  apoptotic pathway[4]. In 2012, a study by Takahashi et al showed that knockdown of FAM129B in mice delayed wound healing compared to controls [5]. This observation corroborates the notion that FAM129B is involved in cancer cell invasion since both processes rely on increased cell mobility, In 2014, a study showed that FAM129B plays a role in the wnt/ $\beta$ -catenin pathway, a pathway well-known to be upregulated in cancer cells[6]. The study, also showed that knockdown of FAM129B promotes apoptosis in melanoma cells, a strikingly different

observation than what was observed in our lab. Finally, in January 2016, a study showed that FAM129B has a tyrosine phosphorylation site (Y593). This tyrosine is phosphorylated by the epidermal growth factor receptor (EGFR). Phosphorylation of FAM129B at this site promotes the binding of FAM129B to H-ras and K-ras, which in turn, promotes glycolysis – part of the Warburg effect in cancer[7].

## **1.2 Domain Structure of FAM129B.**

FAM129B, according to the NCBI databases, exists in two isoforms in Homo Sapiens. Isoform 1 which is made up of 746 amino acids and isoform 2 which is made up of 733 residues. Both isoforms are completely identical in conserved domains and phosphorylation sites with the exception that isoform 1 has an additional 13 amino acid at the amino terminus.

At the amino terminus, FAM129B has a Pleckstrin Homology (PH) domain. This domain has been shown to interact with phospho-lipids at the membrane and is involved in many signaling cascades[8]. This domain also could explain why FAM129B is associated with the Adherent Junctions. At the carboxyl end of FAM129B, there is a tyrosine phosphorylation site (Y593) and a proline rich domain that has six serine phosphorylation sites ( ser628, ser633, ser652, ser668, ser679, ser683). Four of the sites ( ser628, ser633, ser679, ser683) are phosphorylated directly by MAP kinase, while the phosphorylation site for the other two serines remains unknown. Old et al has shown that treatment of melanoma cells with MEK inhibitors relocates FAM129B to the plasma membrane[3]. This observation implies that phosphorylation of FAM129B by MAP kinase regulates FAM129B localization. FAM129B has a DLG and ETGE motif upstream of the proline rich domain. These

domains are conserved in many different proteins, such as NRF2 (nuclear factor protein 2), which is a basic leucine zipper transcription factor that regulates the expression of anti-oxidant proteins that are activated when cells are exposed to oxidative damage[9]. Another protein is IKK $\beta$  (Inhibitor of Nuclear Factor Kappa B Kinase), which phosphorylates the regulatory domain of the protein NF- $\kappa$ B (nuclear factor kappa B), and promotes the transactivation and translocation of NF- $\kappa$ B to the nucleus and transcription of anti-apoptotic proteins and proteins involved in cell proliferation[10]. The expression of both proteins is regulated by KEAP1 (Kelch-like associated protein 1). KEAP1 binds to these proteins through its KELCH repeats to the ETGE domain of these proteins and targets them for degradation by the proteasome[9]. The domain structure of FAM129B is further illustrated in Figure 1.1

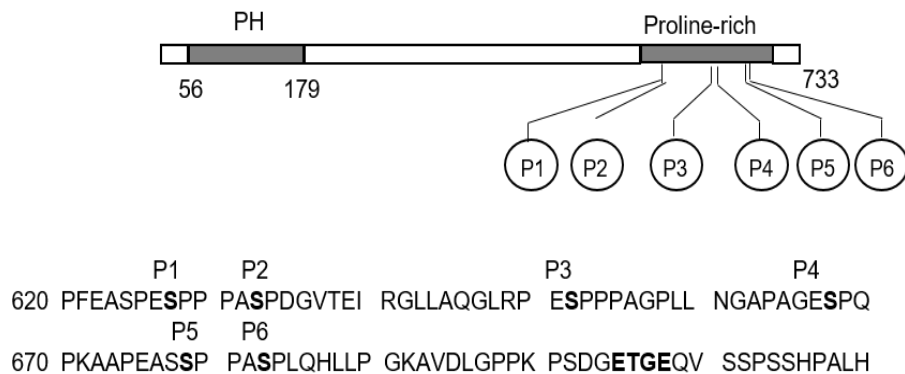


**Figure 1.1:** Domain Structure of FAM129B

### 1.3 Apoptosis

Apoptosis is one type of programmed cell death (PCD). Other types of PCDs include autophagy and programmed cell necrosis. Apoptosis is characterized by certain biochemical and morphological traits. Morphological traits include cellular shrinkage, membrane blebbing, and chromosome condensation. Apoptosis can be induced by a loss of a positive signal, for example, lack of growth factors, or a receipt of a negative signal, for instance, DNA damage or a death ligand. Apoptosis is a highly regulated cellular process. Dysregulation in the apoptotic pathway is associated with many diseases including cancer[11]. Weingburg and Hanahan characterized the suppression of apoptosis as one of the major hall marks of cancer[12]. There are two distinctive apoptotic pathways: the intrinsic or mitochondrial pathway and the extrinsic or death ligand pathway[13].

In the intrinsic pathway(Figure 1.2), cytochrome C is released from the mitochondria with the aid of some proteins from the bcl-2 family and form the apoptosome with a protein called Apaf-1. The apoptosome is then used as a platform for activating the

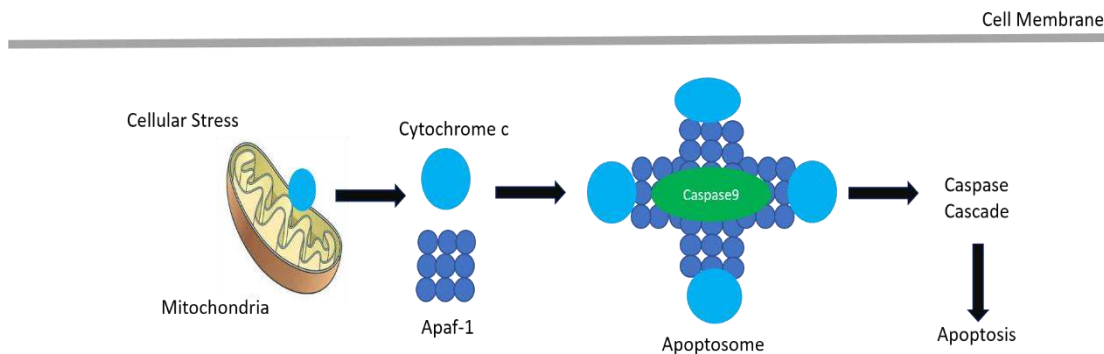


**Figure 1.2. Intrinsic or Mitochondrial Apoptotic pathway**

initiator caspase 9. Caspase 9 activates the executioner caspase 3 and then apoptosis proceeds irreversibly[14].

The extrinsic pathway of apoptosis involves a death ligand docking to a death receptor. There are many types of death ligand and receptors. Two of the most studied are Fas-mediated apoptosis and TNF $\alpha$  mediated apoptosis. In the Fas mediated apoptosis (Figure 1.3), the fas ligand binds to the Fas-receptor. This induces a conformational change that enables the recruitment of FADD adaptor proteins, forming the DISC, the death inducing signaling complex. Once the DISC is formed the initiator caspase 8 is then recruited to the complex and activated. Caspase 8 then proceeds to activate the executioner caspase 3 and apoptosis proceeds[15].

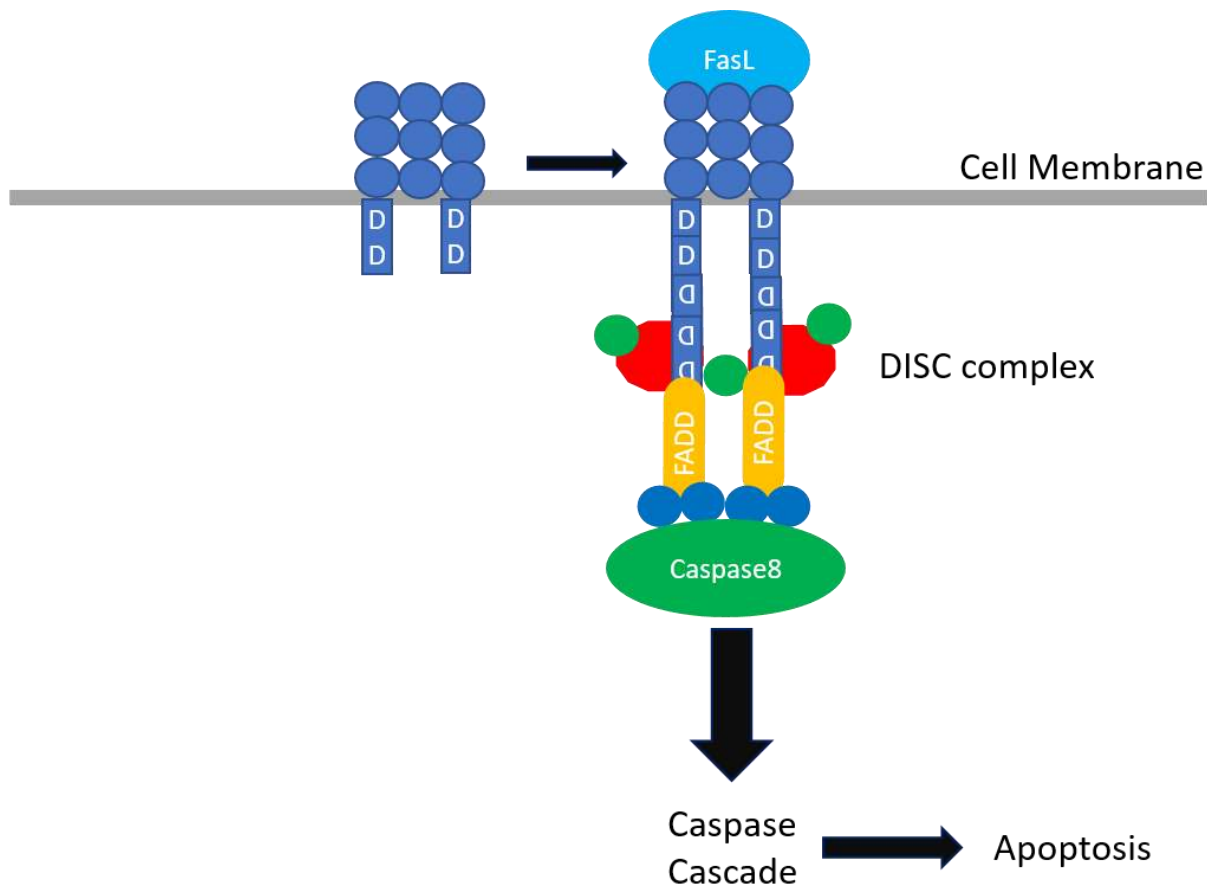


**Figure 1.3: The Fas-mediated Apoptotic Pathway.**

The other well studied extrinsic apoptotic pathway is the TNF $\alpha$  pathway(Figure 1.4). TNF $\alpha$  (tumor necrosis factor  $\alpha$ ), is a cytokine that binds to the TNF receptor. Once bound to the receptor, it forms complex I which is bound to the membrane. Complex I then dissociates from the membrane and the FADD adaptor proteins bind to the complex along with other adaptor proteins. The enlarged complex now designated complex II, forms the DISC, the platform for activating caspase 8. Caspase 8 then activates other executioner caspases and apoptosis proceeds [11]. The TNF $\alpha$  pathway also activates the NF- $\kappa$ B pathway. NF- $\kappa$ B (nuclear factor kappa B) is a transcription factor that activates the transcription of proteins involved in proliferation and cell survival including the IAP family of proteins which are reported to be inhibitors of apoptosis[16].

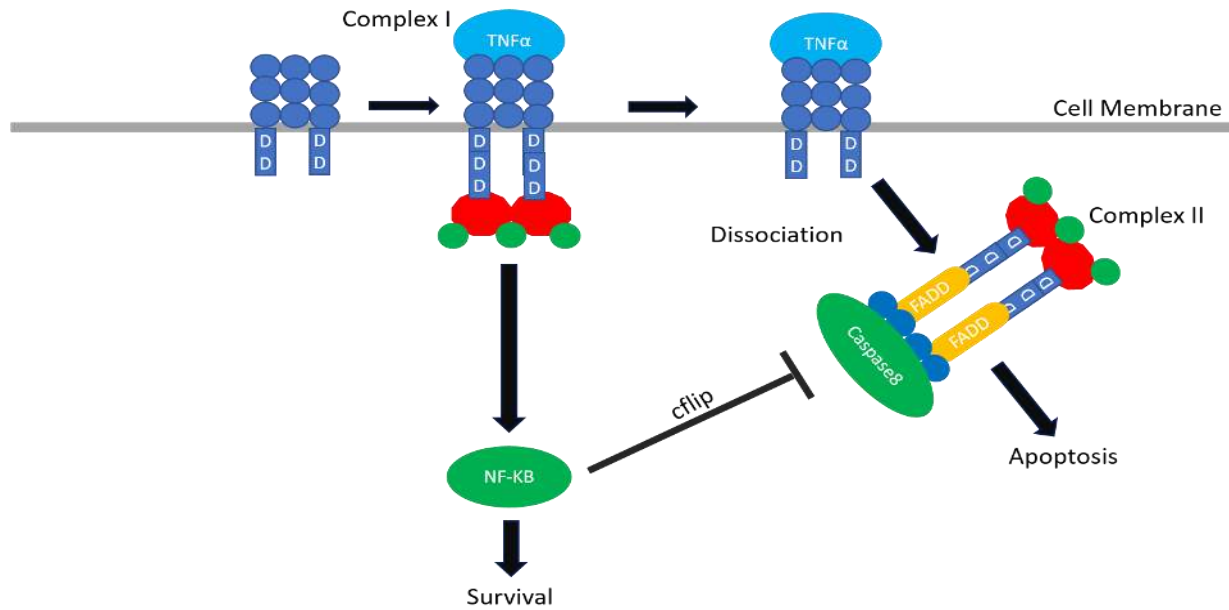


**Figure 1.4: The TNF $\alpha$  Apoptotic Pathway**

Suppression of apoptosis is one of the hall marks of Cancer[12]. Many chemotherapies involve using the death ligands to induce cancer cell death. Also, many anti-apoptotic proteins have been used as drug targets. Small molecules targeting various components of the apoptotic pathway have been already developed. Examples of these molecules are: ABT-737 and ABT-263 have been reported to act on the BCL-2 family proteins. AT-406 and HGS-1029 are thought to antagonize cIAPs[13]

#### 1.4 Cancer and Metastasis

Cancer is a group of diseases where abnormal cellular growth and proliferation occurs to form tumors which have the potential to spread and invade to other parts



of the body. Over 100 types of cancers affect humans. As reported in 2010 by the NCI (National Cancer Institute), 14.1 million cases occur globally. Cancer is the cause of around 14.6% of human deaths. The most common types of cancer in males are lung cancer and prostate cancer while in females, the most common types are breast and cervical cancer[17].

Weinberg and Hanahan published a review in 2011 that summarizes the characteristics of cancer, which they named the cancer hallmarks. The cancer Hallmarks are[12]:

1. Sustaining Proliferative Growth
2. Evading Growth Suppressors
3. Activating Invasion and Metastasis
4. Enabling Replicative Immortality
5. Inducing Angiogenesis
6. Resisting Cell Death

Metastasis is the process where the primary tumor undergoes genetic and biochemical changes that cause the tumor to detach from the primary site and form colonies at a secondary site[18]. Metastasis are very common at later stages of cancer – 90 % of cancer deaths are due to metastatic tumors[17]. The spread of metastatic tumors can occur via both the blood stream and the lymph nodes. The most common site of metastasis are lung, liver, brain, and the bones. For the metastatic spread to occur, primary site tumors induce angiogenesis, which is the process of blood vessel formation. The malignant cell then breaks away from the

primary tumor by degrading the proteins that attach it to the extracellular matrix (ECM) such as cadherins. The malignant cells then enter the blood stream and circulates the bloodstream until they adhere to the blood vessel wall and exit the blood stream and form the colony at a secondary site[19]. The location for metastases is not random since different types of cancer tend to spread to particular and specific organs. An example is breast cancer. Breast cancer primary tumors tend to choose lungs and bones as their metastatic site[20]. This specificity is mediated by signaling molecules such as cytokine or chemokines and TGF $\beta$  (transforming growth factor beta)[21].

Cellular processes that promote cell motility seem to be mostly upregulated in cancer cell metastasis. One example is the Epithelial to Mesenchymal Transition. EMT is critical to morphogenesis and homeostasis of solid tissues. In cancer, malignant epithelial cells undergoing EMT acquire properties that facilitate metastatic spread. EMT renders cancer cells resistant to different types of therapies, often by reducing apoptotic sensitivity. One of the proteins that is down-regulated during EMT is E-Cadherin and the Adherent Junctions are one of mostly altered proteins in Invasive tumors[18].

### **1.3 Significance and Aims**

Cancer is the second leading cause of death in United States. Most of the deaths that occur in cancer are due to metastatic tumors which happen at the later stages of the disease and are resistant to most cancer therapies[17]. Therefore, developing new therapies for cancer is essential. FAM129B suppresses apoptosis and promotes cell mobility. Also, FAM129B is highly expressed in tumor cells. Thus, studying the structure

and function of FAM129B will help in understanding one of the mechanisms by which cancer cells evade death and metastasize, which will lead to life-saving advances in cancer treatment. Furthermore, FAM129B could be a potential drug target for some types of cancer since the loss of FAM129B in cancer cells sensitizes cells to apoptosis and inhibits invasion, which will aid in the development of new cancer therapies and most importantly treatments for metastatic cancers.

Cancer progression is a highly complex mechanism that has yet to be understood, despite decades of research. In our proposed research, we show that FAM129B is involved in cancer cell progression. It suppresses apoptosis and promotes metastasis. Thus, knowing more about FAM129B and its function will give an insight into the mechanisms cancer cells utilize to progress. This will lead to new research approaches and more developments in cancer research and understanding the complicated mechanisms involved in cancer. Therefore, my aims addressed in this thesis are

1. Structural Characterization of FAM129B
2. Characterizing the interaction between FAM129B and KEAP1
3. The role of FAM129B in cancer cell invasion and metastasis

## CHAPTER 2

### MATERIALS AND METHODS

#### 2.1 Vectors used in this Study

All vectors in this study were cloned in our lab. FAM129B was cloned into T7 Sumo Expresso vector which has a Histidine tag and Sumo tag at the amino-terminus (Lucigen). This clone was used to express FAM129B in *E. coli* and purify recombinant FAM129B. FAM129B was also cloned into a pEFGP-n3 vector, which has GFP (Green fluorescent Protein) tag at the carboxyl terminus of the protein . This clone was used to express FAM129B in mammalian cell culture. KEAP1 was cloned into a pDEST15 vector which incorporates a GST tag at the amino-terminus of the protein. This clone was made to express KEAP1 in *E. coli* and to purify the protein

#### 2.2 PCR and Cloning

Invitrogen Gateway Technology was used to clone KEAP1 into pDest15 . Gateway Technology is a highly efficient and fast way to clone genes into multiple expressing systems for functional studies and protein expression. The target gene is first cloned into an Entry vector. The insert of the ENTRY clone can then be recombined efficiently to a destination vector by a ligation reaction. The target gene was amplified by PCR and cloned in a pENTR SD-TOPO vector according to the manufacturer's protocol. The vector was then transformed into TOP10 competent cells and plated on LB agar plates using kanamycin as a selection marker. The vectors were then purified using the Quick plamid mini-prep kit from Invitrogen. The insert in the Entry clone was recombined with

the destination vector according to the manufacturer's protocol. The final vector was checked for the fidelity of the insert via sequencing (Genscript, Piscataway, NJ)

### **2.3 Agarose Gel Electrophoresis**

The HOEFER mini DNA electrophoresis apparatus was used for DNA samples. 0.8% or 1% agarose was made in 1xTAE buffer (40mM Tris base, 0.1% acetic acid, 1mM EDTA, pH 8.0) . The agarose was dissolved in the buffer by heating the solution in the microwave at 30 second increments until the agarose was completely dissolved. The agarose was cooled down and 3 ul of Ethidium Bromide was added. The agarose solution was then poured into a gel casting tray and a 1.5mm 10-well comb was inserted to form the loading wells. The gel was then allowed to solidify at room temperature and placed in the apparatus filled with TAE buffer. Samples were prepared by mixing 5 µl of DNA with 1 µL of 6x loading buffer (Catalog# B7021S, New England Biolabs). The samples were loaded into the wells, along with a DNA standard, 1 Kb plus or 100 bp ladder from New England's Biolabs. The agarose gels were run at 90-100V until the bromophenol blue dye ran approximately 3/4 of the length of the gel. The DNA fragments were then viewed and photographed using a UV-transilluminator.

### **2.4 Cell culture**

HEK293, HeLa, and A549 cells were used in the course of this study. HEK293 is a human embryonic kidney cell line that is widely used for transient transfection studies due to its high transfection efficiency. This cell line was maintained in DMEM media supplemented with 10 % fetal bovine serum (FBS).

HeLa cells are a cervical cancer line. This cell line is the most used cell line in world research due to its robustness and ease of culture. HeLa cells are used for apoptosis studies and immunofluorescent microscopy. HeLa cells were maintained in DMEM media with 10% FBS

A549 cells are a type of lung cancer line. They are epithelial cells. This cell line is widely used to study epithelial to mesenchymal Transition (EMT). This cell line was maintained in RPMI 1640 media supplemented with 10 mM L-glutamine and 10 % FBS.

All cells were maintained in T75 flasks at 37°C with 5% CO<sub>2</sub> in a humidified environment. The media (10 mL) was changed every other day.

Cells were sub-cultured at 80-90% confluency. The media was aspirated and cells were washed once with Phosphate Buffered Saline (PBS). The cells were then incubated with 4 ml of 0.25% Trypsin-EDTA (Invitrogen) until the cells detached from the bottom of the culture flask. The cell suspension was then transferred to a 15 ml sterile tube and 4 ml of Complete media was added to inhibit Trypsin activity. Cells were pelleted by centrifugation at 2000g for 10 min. The media was then carefully removed and the cells were resuspended with 4 ml of complete media. The cells were then seeded in either 6-well plates, 60 mm dishes ,or 100 mm dishes for experimental purposes. For experiments that required accurate cell counts , the cells were counted using a hemocytometer, and the appropriate number of cells were seeded in the experimental flask.

## **2.5 Freezing and Thawing culture cells**

Cells grown to 80-90% confluence in a 75 cm<sup>2</sup> flask, were treated with 4 ml trypsin in a 37 °C incubator. 4 ml growth medium with 10 % FBS were then added to inhibit trypsin activity. The mixture was transferred to a 15 ml sterile tube and centrifuged at 2000g for 10 min at room temperature to pellet the cells. The cell pellet was re-suspended in 2 ml freezing medium (complete) growth medium with 10% (v/v) DMSO. Aliquots of 1 ml (3x10<sup>6</sup> cells) were placed in foam boxes at -80°C overnight and then immersed in liquid nitrogen the next day . Cells were recovered from the nitrogen tank by rapid thawing in a 37°C water bath, and then immediately re-suspended in the appropriate culture medium and transferred to a 75 cm<sup>2</sup> tissue culture flask.

## **2.6 Soluble protein fractions**

Cells grown in plates were washed with PBS (Invitrogen) supplemented with 0.2 mM PMSF (Sigma) and then lysis buffer (20 mM Tris-HCl, pH 7.5, 137 mM NaCl, 1% Triton X-100, 10% glycerol, 0.2 mM PMSF) supplemented with a 1X cocktail of phosphatase and protease inhibitors (Sigma) was added and the cells were incubated on ice for 20 minutes. The cells were then scraped and the sample was collected into a pre-chilled microfuge tube. The cells were vortexed at maximum speed for one minute and the tubes were rotated in the cold for 20 min. The cell lysate was centrifuged for 15 min at maximum speed. The supernatant was designated the soluble fraction.

## **2.7 Sodium dodecyl sulfate-Polyacrylamide gel electrophoresis (SDS-PAGE)**

. The Novex Secure Lock cell from Invitrogen was used for Resolving SDS-PAGE gels. Running gels consisted of a 12 % separating gel and 4% stacking gel. The

electrophoresis buffer contained 0.192 M glycine, 0.025 M Tris-HCl, pH 8.3 and 0.1% SDS. Proteins (1-5 ug) or protein samples (25-100 ug ) were heated for 5-10 min at 70°C in 1 X SDS sample buffer with 20% 2-Mercaptoethanol . The electrophoresis was carried out at a constant voltage of 140 V until the dye front reached the bottom of the gel. The gel was then either subjected to a western blot or stained in 0.05% Coomassie Brilliant Blue R reagent in 45% (v/v) methanol, 9% (v/v) acetic acid in distilled water for 15-30 min, and de-stained in 30% (v/v) methanol, 7.5% (v/v) acetic acid in distilled water.

## **2.8 Western blotting**

Samples were resolved by SDS-PAGE. The gel was then transferred to 0.45 µm pore-size nitrocellulose membrane (Bio-Rad) using a HOEFER transfer apparatus. The filter blotting paper (BioRad) and the nitrocellulose membrane (BioRad) were soaked in transfer buffer. A sandwich was then assembled (foam sponge, filter paper, gel, nitrocellulose membrane-filter paper, foam sponge) making sure to exclude any air bubbles. The sandwich was placed in a transfer tank filled to the required mark with transfer buffer (0.192 M glycine, 0.025 M Tris-HCl, pH 8.3), with the nitrocellulose membrane facing the negative electrode. The transfer was run at a constant current of 400 mA for 90-120 min. The membrane was blocked using a 5% milk solution in 1x TBST (10mM Tris, pH 7.4, 150mM NaCl, 0.1% Tween 20) at room temperature for one hour. The membrane was washed with TBST 3 times and incubated with primary antibody diluted with 5 % BSA with TBST or 5 % milk with TBST. Incubation was carried with gentle shaking, overnight in the cold room. The membrane was then washed three times with TBST at 5 min increments. It was then incubated with a secondary antibody



coupled to Horseradish Peroxidase (HRP) diluted in TBST-milk for 1 hour at room temperature with rocking . The membrane was then washed three time with TBST. The membrane was then incubated with a mixture of the Chemiluminescent Substrate from Bio-Rad for 5 min at room temperature without shaking and with the limited exposure to light.. The signals were obtained by exposing the membranes to UltraCruz™ Autoradiography Film, Blue, sc-201697 (Santa Cruz) from 20 seconds to 10 minutes depending on the intensity of the signals. The films were developed by putting them in a Developer solution for no more than 5 seconds and a Fixer solution (5X stock Developer, Cat#190-0984 and 5X stock Fixer, Cat#190-2485, Eastman Kodak Co.). The resulting immunoblots were scanned and the images were analyzed by Image Studio software from Licor.

## **2.9 Co-immunoprecipitations**

HEK293 cells grown in 6-well plates were transfected with expression constructs using Lipofectamine 2000. 24 hours post-transfection, the cells were lysed and Immuno-precipitation was performed using the Protein G Immunoprecipitation Kit from Invitrogen following the manufacturer's protocol. The samples were then analyzed by western blot analysis.

## **2.10 Protein expression in *E. coli***

Vectors designed for protein bacterial expression were transformed into BL21-A1 competent cells or BL21 cells from Invitrogen. The cells were plated on LB agar plate for 18-20 hours at 37°C in an incubator. The LB agar plates contained an antibiotic as a selection reagent. The next day, a colony from the plate was inoculated in 5-20 ml LB medium with the appropriate antibiotic inside a sterile conical tube. The tube was

incubated in a shaker at 37 °C and 200 rpm for 18-20 hours. The overnight culture was transferred to a bigger flask containing LB medium with the appropriate antibiotic. Cells were grown to an O.D of 0.6. Protein expression was induced using either IPTG (Isopropyl  $\beta$ -D-1-thiogalactopyranoside) or IPTG and L-Arabinose. After induction , the flasks were incubated in a shaker at 20°C and 200 rpm for 18-20 hours. The flasks were then removed from the shaker and the cells were transferred to centrifuge tubes. The cells were pelleted by centrifugation at 6000 rpm at 4 °C for 30 min . The supernatant or the LB was discarded . The mass of the cells were recorded using a balance and cells were stored at -80 °C .

### **2.11 Bacterial Cell lysis**

Cells were resuspended in the appropriate lysis buffer. Lysozyme and Halt-Cocktail protease tablet inhibitors (ThermoFisher) were added to the resuspended cells . The cells were then incubated on ice for 30 minutes . After incubation, the cells were sonicated 3-4 times with 15 second pulses and 1 minute cooling cycles. The lysate was centrifuged at 6000 rpm for 30 minutes. The supernatant and the pellet were separated into different tubes. The supernatant, which contains the soluble protein fraction, was then used for protein purification.

### **2.12 Recombinant Protein Purification**

Recombinant proteins in this study either had a Histidine Tag or a GST tag at their amino terminus. These proteins were purified via affinity chromatography. Poly-Histidine tags have an affinity for Nickel ions , so Pro-bond Nickel resin from invitogen was used to purify proteins with a His-tag. GST has an affinity for glutathione so Glutathione resin from Pierce was used to purify GST-tagged proteins.

### **2.13 Buffer Exchange and Protein Concentrating**

Purified protein fractions were subjected to buffer exchange to get rid of excess Imidazole or glutathione. Desalting columns from Pierce Chemical Co. were used for this process. The columns were washed 5 times with water and then 5 times with the appropriate buffer for the protein. The purified protein fractions were added to the column. The flow through was collected in a tube. Then, the protein was eluted by washing the column with appropriate buffer for the protein. The elutions were collected in 1 ml fractions. The fractions were analyzed for protein presence via Bradford Assay. The samples that contained the protein were transferred to a Concentrator tube with 10,000 molecular weight cut-off(Millipore). The Concentrator tube was centrifuged at 5000 rpm until the volume of the protein solution was 1 ml . The pure protein sample was then transferred into a microfuge tube and stored at -20°C .The concentration of the protein was determined by the Lowry protein assay.

### **2.14 GST-Pull down Assay**

The Pull-down Assay is an *in vitro* method used to determine physical interactions between two or more proteins. The GST pull down Assay Kit was purchased from Pierce Thermo-scientific. Gluthione resin is added to a spin column and washed 5 times with 1:1 TBST Saline Buffer: lysis buffer Solution. The Bait protein (GST-tagged protein) is then added to the Glutathione resin and incubated for 1 hour at 4 °C on a rocking platform to allow the protein to bind. The protein bound resin is then washed 5 times with 1:1 TBST saline buffer : lysis buffer solution to remove any non-specific bindings . The prey protein is then added to the column and the column is incubated for 2 hours at 4 °C on a rocking platform to allow the prey protein to bind to the bait protein. After

incubation, the protein complex is eluted with glutathione. The elution fraction is then analyzed via western blot using the appropriate antibodies to confirm the protein protein interaction.

## CHAPTER 3

### STRUCURAL CHARACTERIZATION OF FAM129B

#### 3.1 Introduction

FAM129B is a 73 Kilobase gene located on Chromosome 9 in homo-sapiens according the NCBI data. The sequence is conserved in a variety of different species as dog, chimpanzee, and rat. FAM129B expression patterns of different cell lines analyzed by immunoblotting in our lab (data not shown) has shown that FAM129B is highly expressed in tumor cell lines compared to non-cancer cell lines. The expression seems to be also higher in metastatic cells lines compared to non-invasive cancer cell lines[22].

FAM129B belongs to a family of proteins of unknown function and structure. Not much is known about FAM129B besides the fact that it is involved in cancer cell invasion and suppression of apoptosis, which are the two of hall marks of Cancer. Therefore, FAM129B exclusive expression in cancer cell lines and its involvement in cancer cell progression highlight the use of FAM129B as a potential biomarker for cancer and also a potential therapeutic target.

Knowing the structure of a protein can lead to implications about the function of the protein. Also, knowing the structure will facilitate the design of a potent and specific inhibitor for FAM129B using structure based drug design.

The domain structure of FAM129B includes a Pleckstrin homology (PH) domain at the N-terminus and a proline-rich domain that has 6 serine phosphorylation sites at the C-terminus along with conserved DLG and ETGE motifs.

In this Chapter, I will show how I expressed and purified FAM129B and seleno-methionine labelled FAM129B. I will also show some in-vitro characterization analysis of FAM129B protein, such as circular dichroism and analytical gel filtration.

## **3.2 Materials and Methods**

### **3.2.1 Expression of FAM129B.**

FAM129B was previously cloned into the T7 Expresso Sumo vector from Lucigen Corp. (Middleton, WI). The plasmid was then transformed into BL21.DE3 cells which are used for expression of proteins in *E. coli*. The next day, a colony was picked (or an aliquot of glycerol stock) was inoculated in 5 ml Luria Broth (LB) media with kanamycin ( 50 µg/ml) as a selection marker. The culture was grown overnight at 37°C with shaking at 200 rpm for no more than 18 hours. The 5 ml overnight culture was then added to the large expression culture (500 ml) LB media and kanamycin. The cells were then grown at 37°C with shaking at 200 rpm until the optical density at 600 nm reached 0.5-0.6 which occurs in 3 to 4 hours. Protein expression was induced with IPTG at a final concentration of 0.5 mM. The cells were then left to grow at 20°C at with shaking at 200 rpm for 18 hours. The cells were then centrifuged at 4000xg for 30 minutes to remove LB media. The cell mass was determined by an analytical balance and was either processed immediately or stored at -80°C until needed.

### **3.2.2 Expression of Seleno-methionine labelled FAM129B (Sel-met FAM129B).**

Cultures were grown and processed with the same steps in the above section 3.2.1 until induction when the O.D. had reached 0.60. The cells were then pelleted by centrifugation and gently mixed with methionine-free M10 minimal media (4g NH<sub>4</sub>Cl, 12g KH<sub>2</sub>PO<sub>4</sub>, 24 g NaH<sub>2</sub>PO<sub>4</sub> 1g Magnesium sulfate ,0.05 g Ferrous sulfate in 500 ml of distilled water). The cells were then resuspended with 500 ml of M10 media supplemented with vitamin supplements, glucose, all amino acids except for methionine and 50 mg of seleno-methionine. The culture was incubated in the shaker at 37°C and rotated 200 rpm until the O.D 600 reached 0.6. The culture was then induced with IPTG added to a final concentration of 0.5 mM and the cultures were then incubated for 16-18 hours at 20°C shaking at 200 rpm. The cells were then pelleted by centrifugation.

#### **3.2.4 Purification of FAM129B.**

Cell pellets from the previous section were re-suspended in purification buffer (50 mM Sodium Phosphate pH 8.0, 500 mM NaCl ) at a ratio of 5 ml/g of cell pellets. The cells were gently suspended and protease inhibitor was added to the cell suspension. The cells were incubated on ice for 30 min. The cells were lysed by sonication on ice at 30 second intervals with 3 minute cooling in-between 3 to 4 times. The cell lysate was then centrifuged at 6000 rpm for 30 min at 4°C. The supernatant containing the soluble protein including FAM129B was separated from the pellet by decanting. The supernatant was then loaded on a column containing 2 ml of Nickel resin. This step is the binding step where the His-FAM129B binds to the Nickel column and all other bacterial proteins are – hopefully – eluted and collected, as the “flow through”. The column was washed 3 times with 20 mM Imidazole in purification buffer. The

recombinant protein was then eluted with 250 mM Imidazole in fifteen 1 ml fractions. The pellet, supernatant, flow-through, the three washes, and the elutions were analyzed by SDS page gel. The elutions were then pooled together and the protein was concentrated down to a 1 ml volume using Millipore concentrators. The protein concentration was determined by the Lowry Assay. For CD analysis and crystallization, FAM129B was passed through a gel-filtration column (S-300) to further clean up any impurities. The fractions were then concentrated and the protein concentration was determined.

### **3.2.5. Gel filtration of FAM129B**

1 ml of concentrated (20 mg/ml) of FAM129B was loaded onto the Bio-Rad gel filtration system using 280 ml of S300 resin. The program was run at a flow rate of 1 ml/min collecting a total of 320 ml of buffer (50 mM Tris pH 8.0, 200 mM NaCl ,1 mM DTT) in 4 ml fractions. A molecular weight standard from Bio-rad consisting of thyroglobulin (670 kDa),  $\gamma$ -globulin(158 kDa), ovalbumin (44 kDa), Myoglobin (17 kDa) and Vitamin B12 (1.35 kDa) was run on the same column and Log MW was plotted against the volume of when the protein was eluted. The FAM129B oligomerization state was then determined from the standard plot.

### **3.2.6 Circular Dichroism Analysis.**

Purified FAM129B was buffer exchanged into 1 mM Sodium Phosphate buffer pH 7.5 at a final concentration of 2.4  $\mu$ M. The sample (400  $\mu$ L) was loaded into a 0.1 cm cuvette and inserted into the Circular Dichroism Spectrophotometer. Three separate spectra were collected for the sample. The spectra were then accumulated using the JASCO



C.D analysis software. The resultant spectrum was then analyzed using C.D pro-analysis using the parameter *Cotnin*. The alpha helices, beta-sheet, and random secondary structures percentages were then calculated..

**3.2.7 Crystallization Screening of FAM129B.** Purified FAM129B in 50 mM Tris pH 8.0, 200 mM NaCl buffer at a final concentration of 10 mg/ml was screened for crystallization conditions using the classic screen from Jenna Bioscience (JBS) and classic suite screens from Qiagen. The hanging drop method was used for these crystallization screens[23]. Briefly, 1  $\mu$ L of purified protein was mixed with 1  $\mu$ L of the crystallization solution on siliconized microscope coverslip. The cover slip was inverted placed over a well in a 24 well plate with each well containing a 0.5 ml of the different crystallization solutions taking care that chamber was sealed tightly. The screens were then checked under microscope at the time of set-up for any precipitation. The screens were monitored every 3 days over a duration of 1 month. Any conditions that yielded crystals were recorded and repeated for confirmation. The crystals were picked and soaked with cryoprotectant (crystal condition with 20% ethylene glycol) and frozen in liquid nitrogen. The crystals were sent to Argonne National lab Synchrotron in Illinois for data collection.

### 3.3 Results

**3.3.1 Purification of FAM129B** In order to do In-vitro analysis of FAM129B, we first set out to isolate the protein. Bacterial protein expression is a widely-established method to isolate protein in vitro. FAM129B was cloned into a vector with a his-tag at the amino terminus of the protein to enable the isolation of protein using affinity chromatography with a Nickel resin bed as indicated in the methods. The expression and affinity purification gel in Figure 3.1A shows that FAM129B was successfully isolated. The molecular weight of FAM129B is approximately 80 kDa from the gel. FAM129B was gel-filtered by an S300 gel filtration column. The gel in Figure 3.1B shows the final purity of FAM129B that was used in C.D analysis and crystallization.

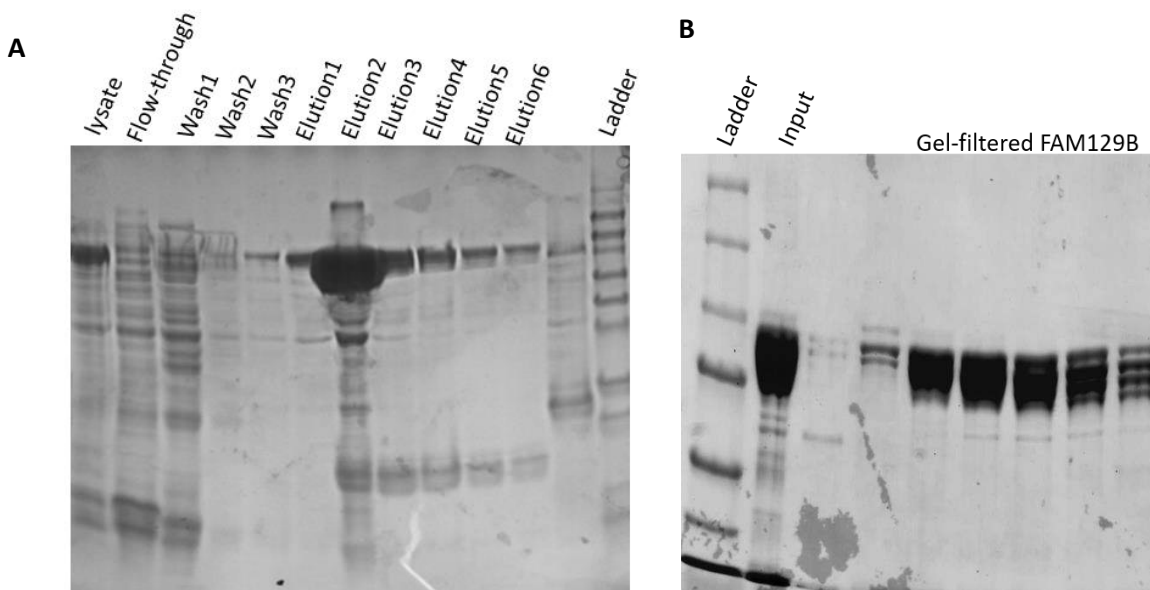


**Figure 3.1. Purification of FAM129B.** (A) Recombinant FAM129B cloned into T7 SUMO vector(lucigen) expressed in E.Coli. The protein was then purified by affinity purification. Samples designated in the figure were ran on 12 % SDS-PAGE to assess the expression and purification of recombinant FAM129B.(B) FAM129B was loaded onto an S300 gel filtration column.The fractions that contained FAM129B were loaded onro SDS-PAGE gel with the input to assess the purity of the fraction

### 3.4.2 Analytical Gel filtration of FAM129B

We wanted to check if FAM129B exists in monomer, dimer, or trimer or any other oligomeric state. Oligomeric state of the protein is associated with the function of protein[24]. Gel filtration is a way of purifying proteins based on size so by comparing to a molecular weight standard, the volume at where the protein elutes will give us an idea about the protein oligomeric state. A sample of FAM129B (1 ml of 20 mg/ml) run on a S300 gel filtration column eluted at 192 ml which corresponds to a molecular weight of 166 kDa, Therefore FAM129B exist as a dimer in solution.(Figure 3.2)

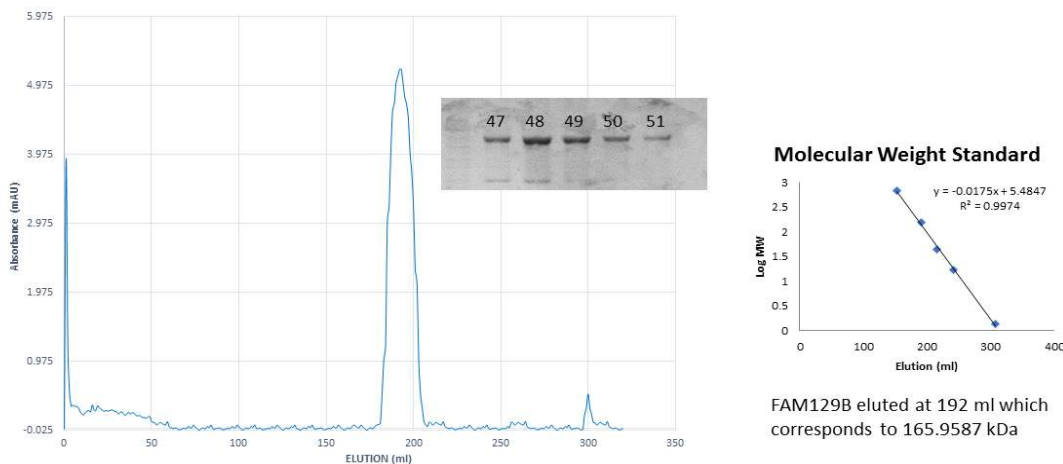


**Figure 3.2. FAM129B exists as a dimer according to gel filtration Analysis.** Recombinant concentrated FAM129B protein was loaded onto S300 Gel filtration column. Fractions were collected at a rate 1ml/min in 4 ml total fraction volume. Fractions that corresponded to the peak were analyzed by SDS-PAGE gel to verify the existence of the protein.

### 3.4.3 Circular Dichroism Analysis of FAM129B<sub>36</sub>

Since FAM129B is a new protein of unknown structure, we thought it would be interesting to run a C.D analysis on the protein. Circular Dichroism Spectroscopy is a method to determine the secondary structure of protein and the percent composition of alpha-helices and beta sheets since they have distinct C.D spectra[25]. The C.D spectra of FAM129B showed that the secondary structure composition is 37% alpha helices, 19 % beta sheets, 22% turns, and 22% undetermined. Figure 3.3 lists the exact values obtained and shows the C.D spectrum of FAM129B.

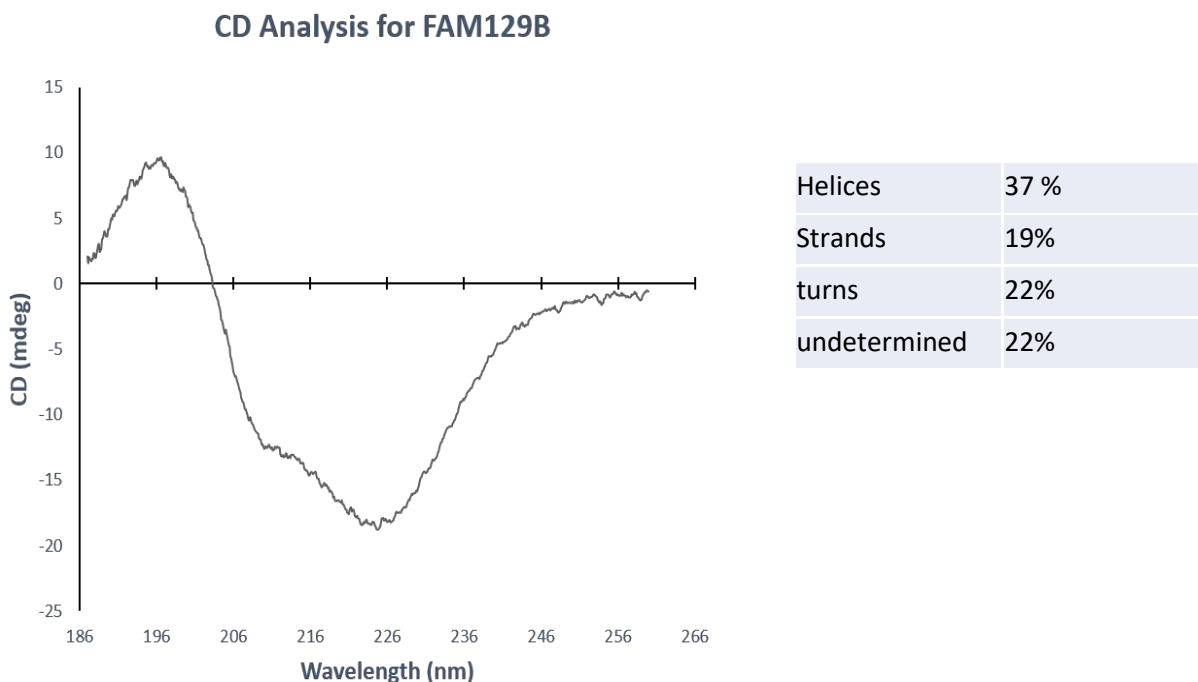


**Figure 3.3. Circular Dichroism Spectra of Purified His-FAM129B** 2.4 $\mu$ M in 1 mM Sodium phosphate buffer was analyzed using a circular dichroism spectrophotometer. The resultant CD spectra above showed the characteristic helix peak at 196 nm and the strand peak at around 226 nm. The percentages of secondary structures are summarized in the table above. The undermined structure is can be indicative of disordered regions.

### 3.4.4 Crystallization Screens of FAM129B

Obtaining a Crystal is the rate limiting step for solving a structure of any protein by X-ray crystallography. Usually, structural biologists must try many different crystallization screens to obtain protein crystals[23]. FAM129B crystallization screens yielded almost no crystals from 2 two different screens representing 500 different conditions (Jenna Bioscience Crystallization Screen and the Qiagen Class Suite Screen). Only one condition from the Qiagen classic screen yielded decent looking crystals. The condition for crystallization is: 0.1M Na<sup>+</sup> cacodylate, pH 6.5 , 30% MPD (2-Methyl-2,4-pentanedio), 0.2M Mg acetate shown in figure 3.4 The crystals were sent to the LS-CAT synchrotron for analysis. However, the crystals obtained turned out to be salt.

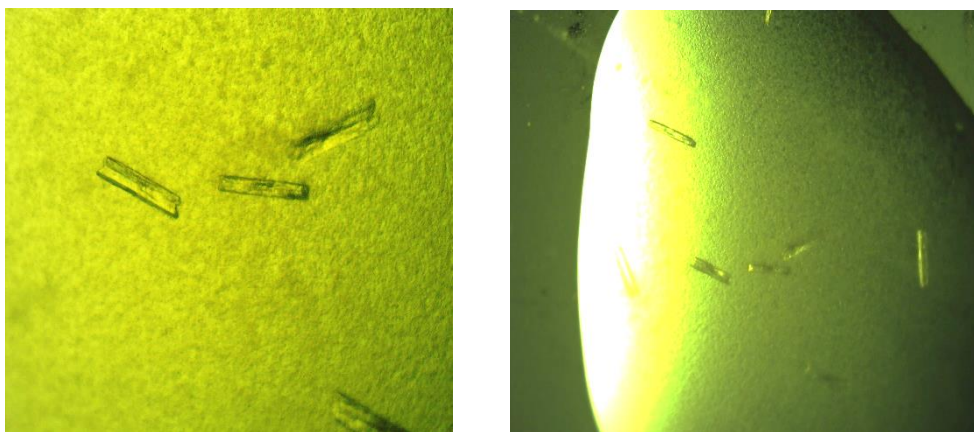


**Figure 3.4. Crystallization Screening Results of Purified FAM129B.** 10 mg/ml of purified recombinant FAM129B in 50 mM Tris ,150 mM NaCl pH 7.5 was used in different crystallization screens. The screens were set-up using the hanging-drop method. The condition above 0.1M Na<sup>+</sup> cacodylate pH 6.5 , 30% MPD , 0.2M Mg acetate. However, they turned out be to be salt and not protein crystals.

### 3.5 Discussion

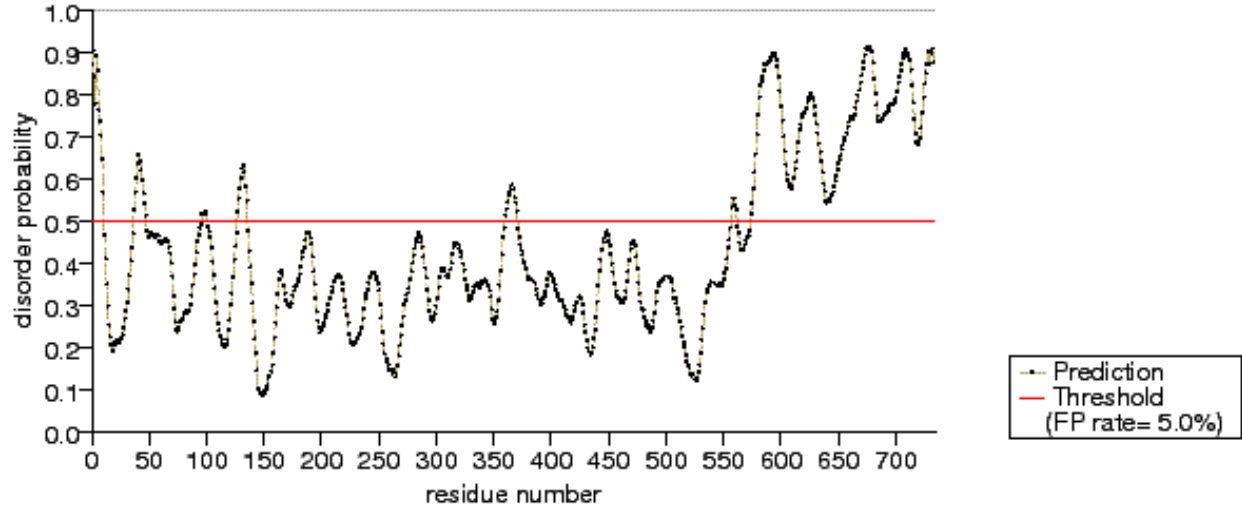
Purification and Isolation of FAM129B from a bacterial expression system and the subsequent analysis has yielded much information about the protein. First, FAM129B is a soluble protein, which supports previous finding that FAM129B is predominantly a cytosolic protein. Also the high solubility of FAM129B highlights the fact that FAM129B might not be an integral part of cell membrane and can shuttle between and the cytosol and the adherent junction as shown by Old et al[3].

The second observation is that FAM129B has been successfully purified at high yields, which facilitates the study of the protein in subsequent studies *in vitro* such as ITC, pull-down assays, and crystallization, which are experiments that require large amounts of protein.

Gel filtration analysis of FAM129B has shown that FAM129B exists as a homo dimer in solution *in vitro*. Oligomeric states of protein can affect the function of the protein[24]. FAM129B has six serine phosphorylation sites and a tyrosine phosphorylation close to the carboxyl terminal of the protein. Since FAM129B was purified from bacteria that have few kinases and do not phosphorylate mammalian proteins, we conclude that the un-phosphorylated protein forms the dimer in this case. An interesting aim would be to see how the different phosphorylation states affect the oligomeric state of the protein and how does that affect FAM129B function as well[3]. Old et al has shown that phosphorylation affects FAM129B localization to membrane. Therefore, if the oligomeric state of the protein of FAM129B is affected by phosphorylation state, then dimerization of FAM129B can also affect FAM129B localization to the membrane and the different

functions that FAM129B exhibits in cancer cell, which include suppressing apoptosis and promoting cancer invasion.

Circular Dichroism spectroscopy is used in the field of biochemistry and protein structure to determine the secondary structure of protein. Around 40 % of FAM129B consists of alpha helices and around 20% of protein composed of beta sheets. Around 22% of the protein seems to be unfolded or has no definite shape. We repeated the analysis 2 times on 2 different batches of the purified protein and we got nearly identical results. Around 22% remains mostly unfolded or undetermined. Secondary Structure Prediction software tools online have shown that almost the entire carboxyl terminus of FAM129B is disordered (Figure 3.5). This prediction agrees with our CD analysis of the protein. Also, the domain structure of FAM129B shows that carboxyl terminal of FAM129B is proline rich and has 7 phosphorylation sites which could be the reason for the high percentage of the undetermined secondary structure and folding of the protein.



(Red: Disordered residues Black: Ordered residues)

1	<b>MGWMGEKTGK</b>	ILTEFLQFYE	DQYGVAlFNS	MRHEIE <b>GTGL</b>	<b>PQAQLLRKV</b>	50
51	PLDERIVFSG	NLFQHQEDSK	KWRNRFSLVP	HNYGLVLYEN	KAAYER <b>RQVPP</b>	100
101	RAVINSAGYK	ILTSVDQYLE	LIGNSL <b>PGTT</b>	<b>AKSGS</b> APILK	CPTQFPLILW	150
151	HPYARHYFC	MMTEAEQDKW	QAVLQDCIRH	CNNGIPEDSK	VEGPAFTDAI	200
201	RMYRQSKELY	GTWEMLCGNE	VQILSNLVME	ELGPELKAEL	GPRLKGGKQPE	250
251	RQRQWIQISD	AVYHMYEQA	KARFEEVLSK	VQQVQPAMQA	VIRTDMDQII	300
301	TSKEHLASKI	RAFILPKAEV	CVRNHVQPYI	PSILEALMVP	TSQGFTEVRD	350
351	VFFKEVTD <b>MN</b>	<b>LNVIN</b> EGGID	KLGEYMEKLS	RLAYHPLKMQ	SCYEKMESLR	400
401	LDGLQQRFDV	SSTS <sup>V</sup> FKQRA	QIHMREQMDN	AVYTFETLLH	QELGKGPTKE	450
451	ELCKSIQ <sup>R</sup> VL	ERVLK <sup>K</sup> YD <sup>Y</sup> D	SSSV <sup>R</sup> K <sup>R</sup> FF <sup>R</sup>	EALLQ <sup>I</sup> S <sup>I</sup> P <sup>F</sup>	LLK <sup>K</sup> L <sup>A</sup> P <sup>T</sup> C <sup>K</sup>	500
501	SELPRFQELI	FEDFARFILV	ENTYEEVVLQ	TVMKDILQAV	KEAAVQRKHN	550
551	LYRDSM <b>VMHN</b>	<b>SDPNL</b> HLLAE	GAP <b>IDW</b> GEEY	<b>SNSGGGG</b> SPS	<b>PSTP</b> ESATLS	600
601	<b>EKRRRAKQVV</b>	<b>SVVQD</b> EEVGL	<b>PFEAS</b> PESPP	<b>PASPDG</b> VTEI	<b>RGLLAQ</b> GLRP	650
651	<b>ESPPP</b> AGPLL	<b>NGAP</b> AGESPQ	<b>PKAA</b> PEASSP	<b>PASPLQ</b> HLLP	<b>GKA</b> VDLGPPK	700
701	<b>PSDQ</b> ETGEQV	<b>SSPSS</b> HPALH	<b>TTT</b> EDSAGVQ	<b>TEF</b>		750

**Figure 3.5 . Disorder Prediction Analysis.** The protein sequence of FAM129B was subjected to a disorder prediction analysis. The results predict that FAM129B has a highly disordered C-terminal region. The disordered residues are labelled in red.

**Source :** Ishida, T and Kinoshita, K, PrDOS: prediction of disordered protein regions from amino acid sequence., *Nucleic Acids Res*, **35**, Web Server issue, 2007



FAM129B Crystallization yielded no hits or good crystals. Crystallization of proteins is dependent on many factors: the buffer of the protein, the crystallization condition, pH , protein concentration , temperature, and the folding of the protein[23] . Even though FAM129B has been produced in high yields. is soluble and is stable in tris and phosphate buffers, the crystallization of this protein was met with unfortunate results. One reason that could be given for the low crystallization hits of FAM129B is the highly disordered carboxyl terminal of protein. Future efforts should be made in dividing the protein in a way that would facilitate crystal packing. Efforts should also be made in crystallizing FAM129B with seleno-methionine residues. Since FAM129B does not have any structurally homologous protein in the Protein Data Bank, molecular replacement cannot be used to solve the structure . So to solve this problem, crystallization of sel-met FAM129B will be necessary to determine the structure of the protein[26]. We have successfully expressed and purified seleno-methionine recombinant FAM129B as shown Figure 3.6 Attempts to crystallize this protein have so far yielded no results.

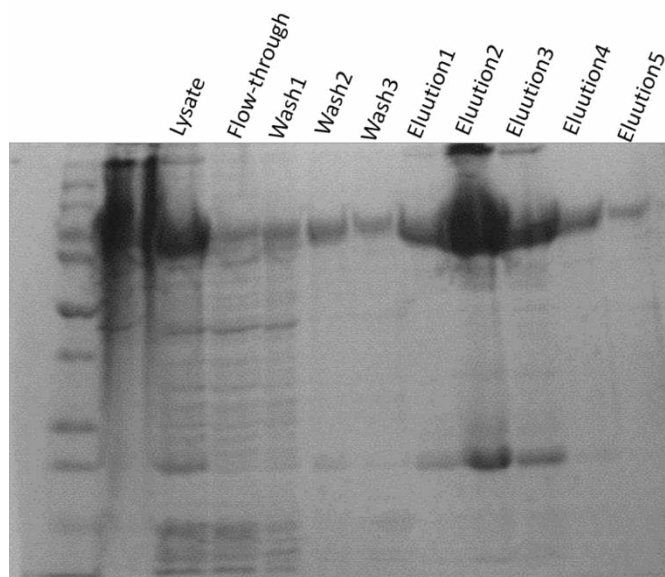


**Figure 3.6. Seleno-Methionine labelled FAM129B Protein Purification gel**

## CHAPTER 4

### CHARACTERIZING THE INTERACTION BETWEEN FAM129B and KELCH-LIKE ASSOCIATED PROTEIN 1, KEAP1

#### 4.1 Introduction

FAM129B has been shown to suppress apoptosis in HeLa cells [4, 22]. Therefore, we sought to identify possible interacting protein partners for FAM129B in the hopes to better understand the mechanism by which FAM129B suppresses apoptosis. Preliminary results in our lab from a Mass Spectrometry Analysis has identified KELCH-like associated protein 1, KEAP1 as a possible interacting partner[22]. The interaction was confirmed by Immuno-precipitation of endogenous KEAP1 with GFP-FAM129B in transfected HEK293 cells[22].

KELCH-like Associated Protein 1, also known as KEAP1, is a 59 KDa zinc protein. KEAP1 is a Cul3 based substrate recognition adaptor. KEAP1 can target proteins for degradation through the Cul3 based ubiquitin ligase. The domain structure of KEAP1 shows that KEAP1 has three distinct domains. The BTB domain at the amino end of the protein is the site of KEAP1 homo-dimerization. Downstream of the BTB domain is the IVR domain, which binds the CUL3 based Ubiquitin ligase. At the carboxyl end of KEAP1 there are 6 KELCH repeats, which interact with proteins that contain an ETGE motif, usually lead to degradation. The KECLH repeats have also been shown to interact with the BH3 domain of BCL-2. The KELCH domain of KEAP1 structure has been solved[27]. The crystal structure shows that six copies of the KELCH repeats form

a beta-sheet propeller where the target proteins are thought to bind into the center of propeller shown in Figure 4.1[28]

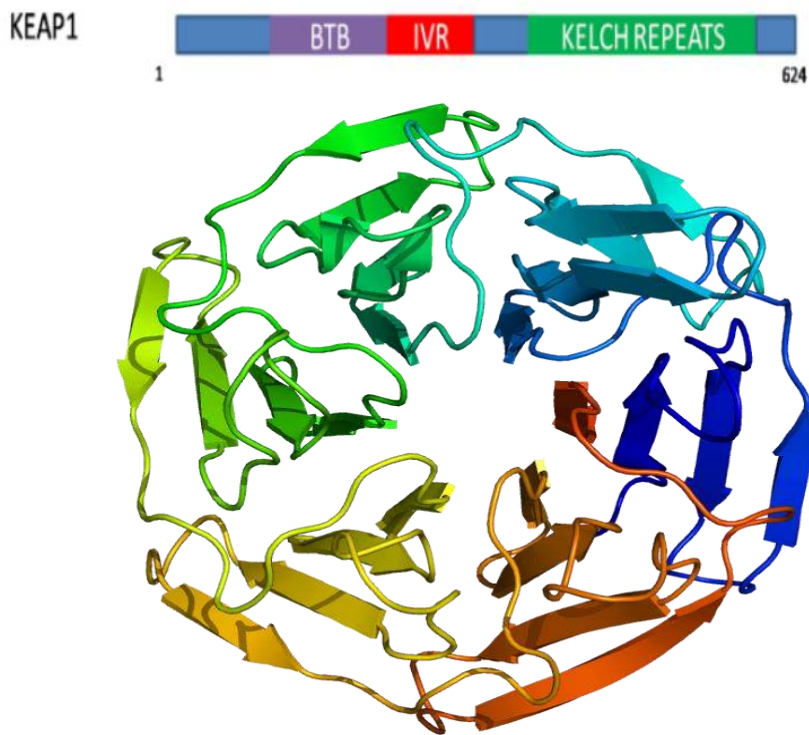


**Figure 4.1. Domain Structure of KELCH-Like associated Protein 1 (KEAP1).**

**Source:** DOI: [10.2210/pdb1u6d/pdb](https://doi.org/10.2210/pdb1u6d/pdb)

One of the most studied targets of KEAP1 is the antioxidant response protein NRF2. Under normal conditions, KEAP1 binds to NRF2 through the KELCH repeats and the ETGE motif respectively and targets NRF2 for degradation. However, upon oxidative stress, KEAP1 -NRF2 complex is disrupted due to the reactive cysteines on KEAP1 and NRF2 is released. NRF2 then translocates to the nucleus and activates the transcription of the anti-oxidant responses protein. This process has been reported to be highly

elevated in cancer cells to promote their survival. KEAP1 inactivation or down regulation has also been reported in different types of cancer, including lung cancer[29].

IKK $\beta$ , also known as Inhibitor of nuclear factor Kappa B kinase, is also a target of KEAP1 mediated degradation. IKK $\beta$  is highly elevated in cancer cells and is recognized as an oncogenic kinase[30]. IKK $\beta$  also activates the NF- $\kappa$ B pathway. NF- $\kappa$ B or nuclear factor kappa B is a transcription factor protein complex that activates transcription of proteins that are involved in cellular growth and survival[10]. Several studies have confirmed the direct interaction between IKK $\beta$  and KEAP1 and that KEAP1 down-regulates IKK $\beta$  binding. These findings show that KEAP1 can down-regulate the NF- $\kappa$ B pathway. This pathway has been reported to be elevated in many types of cancer and NF- $\kappa$ B is considered an attractive drug target for many cancer therapeutics[16].

The NF- $\kappa$ B pathway can be induced by TNF $\alpha$ . Since FAM129B suppresses the TNF $\alpha$  apoptotic pathway in cancer cells, we hypothesized that FAM129B activates the NF- $\kappa$ B pathway by competitively binding to KEAP1 and thus blocking the KEAP1 and IKK $\beta$  interaction and thereby preventing the degradation of the kinase. The working model of our hypothesis is illustrated in figure 4.2

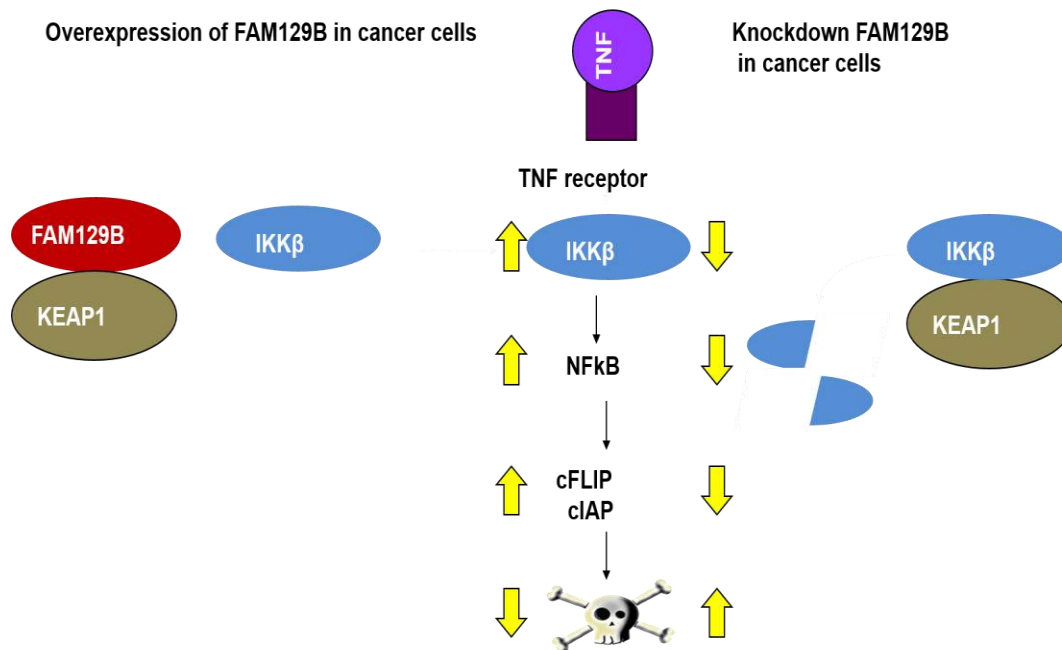


**Figure 4.2. Working Model of Hypothesis.** Overexpression of FAM129B in cancer leads to FAM129B binding to KEAP1, thus preventing the latter from binding to IKK $\beta$ . IKK $\beta$  is then protected from degradation which leads to an upregulation of NF- $\kappa$ B activation which promotes the expression of anti-apoptotic proteins which ultimately leads to the suppression of cell death.

But before further elucidating the mechanism, we have to confirm the interaction between FAM129B and KEAP1. In this chapter I confirm the interaction between KEAP1 and FAM129B through GST pull-down assays. I also identified the sites of interaction between both proteins.

## 4.2 Material and Methods

**4.2.1 PCR and Cloning of KEAP1, KELCH REPEATS AND KEAP1 $\Delta$ KELCH pDEST15.** Gateway Technology from Thermo-Fisher was used to efficiently clone KEAP1 and the deletion constructs into pDEST15 plasmid, which has an amino-terminus GST tag. pcDNA KEAP1 vector was used as the template for the PCR reaction. The primers used for full length KEAP1 , Forward: 5'CACCATGCAGCCAGATCCCAGGCCTAGC, Reverse :5'TCAACAGGTACAGTTCTGCTGGTCAATCTGCTTCCGGCA.

For the KELCH Repeats, Forward : 5' CACCATGGCGCCCAAGGTGGGC. Reverse: 5' TCAACAGGTACAGTTCTGCTGGTCAATCTGCTT . For KEAP1 $\Delta$ KELCH , Forward: 5' CACC ATGCAGCCAGATCCCAGG , Reverse: 5'CTACCGGCAGGGCATCACCTG

Following the PCR reaction, the inserts were then purified using quick PCR clean up kit from Thermo-fisher. The PCR products were cloned into pENTR SD/TOPO plasmid following the manufacturer's protocol. The generated Entry clones were then incubated with the destination vector pDEST15 following the manufacturer's instructions. The newly obtained clones were then verified by DNA sequencing by sending the samples to Genscript , Picastaway , NJ.

### 4.2.2 Protein Expression of GST fused proteins

The GST fusion protein vectors were transformed into BL21-A1 expression strain from Thermo-fisher. The next day, a colony was picked and inoculated into 5 ml LB media with Ampicillin used as a selection marker. The culture was grown for 18 hours at 37°C and shaking at 200 rpm. The overnight culture was then transferred to a 500 ml

LB media with ampicillin. The expression culture was left to grow at 37°C and shaking at 200 rpm until the Absorbance at 600 nm reached 0.5. Protein expression was then induced by adding both IPTG and L-arabinose at a final concentration of 0.5 mM and 0.2 % w/v respectively. Following Induction, the cells were left to grow overnight at 25°C and shaking at 200 rpm for no more than 16 to 18 hours. The cells were then pelleted by centrifugation and the mass of cells was determined. The cell pellet was either used directly for purification or stored at -80°C until needed.

#### **4.2.3 Purification of GST fused proteins.**

GST fusion proteins were purified using Glutathione resin (2 mL). The cells from the previous section were resuspended in purification buffer (50 mM Tris pH 8.0, 150 mM NaCl) at a 5 ml of buffer / 1 g cells ratio. Protease Inhibitors were added and the cells were incubated on ice for 30 min. The cells were then lysed by sonication for at 30 sec intervals with 1 min cooling interval in between 3 to 4 times. The cell lysate was pelleted by centrifugation at maximum speed for 30 minutes. The supernatant was then loaded on to the Glutathione column at a flow rate 20 drops/ min. The GST protein now bound to the column was washed three times with purification buffer. The protein was eluted with buffer containing reduced glutathione (250 mM) , 50 mM Tris , 150 mM NaCl at pH 8.0. The elution volume was collected in ten 1 ml fractions. The samples were the analyzed by SDS-PAGE gel to assess purity of protein. The protein was concentrated down to 1-2 ml volume using Millipore Concentrators and the protein concentration was determined by the Lowry method.

#### **4.2.4 GST Pulldown Assays**

Approximately 150-250 µg of purified GST tagged recombinant proteins were incubated with 25 µg of GST resin for 1 hour at 4°C. The GST resin with bound protein was washed and then 150 µg - 250 µg of purified His-FAM129B was added. The proteins were incubated for 2 hours at 4°C . The protein complexes were eluted and the samples were analyzed using Western blots with His tag and GST tag antibodies.

#### **4.2.5 Immuno-precipitation Experiments**

HEK293 cells were grown in a 6 well plate until they were 60-80% confluent . The cells were then transfected with 2.5 µg of plasmid using Lipofectamine 2000 (Life technologies) . 24 hours post- transfection, the cells were lysed and an immunoprecipitation was performed with a GFP antibody using the G-protein Immunoprecipitation kit (Life Technologies) according to the manufacturer's protocol . The samples were then analyzed via Western Blot using KEAP1 and GFP antibodies ( Cell Signaling).

#### **4.2.6 Immuno-Flourescent Microscopy**

HeLa were plated on glass cover slips and grown to 60-80% confluency. The cells were serum starved overnight and then treated with TNFα (10 ng/ml) for 30 min. The media was aspirated from the well. The cells on the coverslips were then washed with PBS (Phosphate buffered Saline) 3 times. The cells were then fixed with 10% formalin and permeabilized with 0.2% Triton-X. Next, the cells were blocked with 1% BSA in PBS for 1 hour. After blocking, the cells were washed 3 times with PBS. The cells were incubated with antibodies against FAM129B and KEAP1 (1:50) in blocking buffer for 2 hours. After washing the cells 3 times with PBS, the cells were incubated with Alexa



flour 594 Goat anti-Rabbit and 488 Goat anti-mouse for 1 hour. The cells were then washed with PBS. After that, the coverslips were the mounted on clean microscope slides using Prolong Gold Anti-Fade mountant with DAPI (Life Technologies, P36931). The microscope slides were then stored in the dark at 4°C overnight to allow the slides to dry. The cells were analyzed using a fluorescent microscope Nikon E800.

### **4.3 Results**

#### **4.3.1 Cloning of KEAP1 and the Deletion Constructs in pDEST15 vector.**

To perform *In-vitro* GST pulldown, KEAP1 had to be cloned into a GST tagged plasmid. We then divided KEAP1 into two parts so we can examine which domain specifically binds FAM129B. These two parts are the KELCH repeats (GST-KELCH) and KEAP1 without KELCH repeats (GST-KEAP1 $\Delta$ KELCH). The PCR agarose gels of the full length KEAP1 and the truncated constructs show that the PCR reaction was successful (Figure 4.3) The inserts were cloned into the entry clone and then further into the destination vector pDEST15. The resulting clones were confirmed by sequencing to check for two criteria: 1) that the sequence was correct. 2) KEAP1 and the deletion constructs inserts were in frame and properly fused with the GST tag at the amino terminus. The sequencing results showed that both criteria were met for all 3 clones.

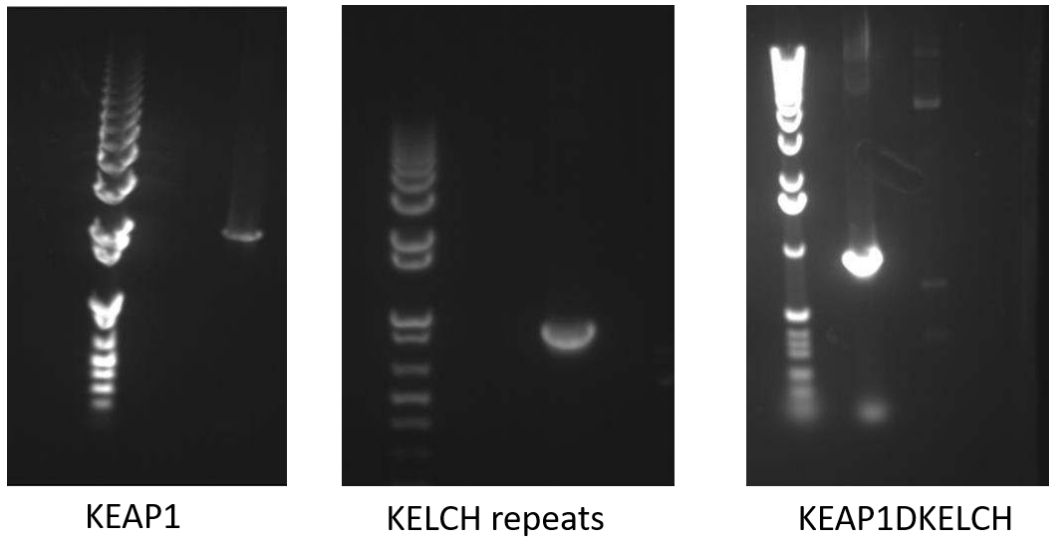


**Figure 4.3. PCR results for the amplification of KEAP1 and the corresponding Deletion Constructs.** 5  $\mu$ L of purified PCR product was mixed with 1  $\mu$ L of 6X loading (New England's Biolab). The samples were resolved on 0.8% agarose gel. Images were taken using UVP gel imager

### **4.3.2 Expression and Purification of GST-KEAP1, GST KELCH Repeats, and GST-KEAP1- $\Delta$ KELCH**

Expression and Purification of GST-KEAP1 was successful. The protein was soluble and was purified as indicated in Figure 4.4. The gel also shows that the molecular weight of GST-KEAP1 is approximately 80 kDa. To further confirm our results, the samples were subjected to Western Blot analysis using both GST tag antibody and KEAP1 antibody. The resulting Immuno-blot showed that KEAP1 was indeed expressed and purified. The purification of both the deletion constructs: GST-KELCH and GST-KEAP1 $\Delta$ KELCH was also successful as indicated in Figure 4.4(D&E)

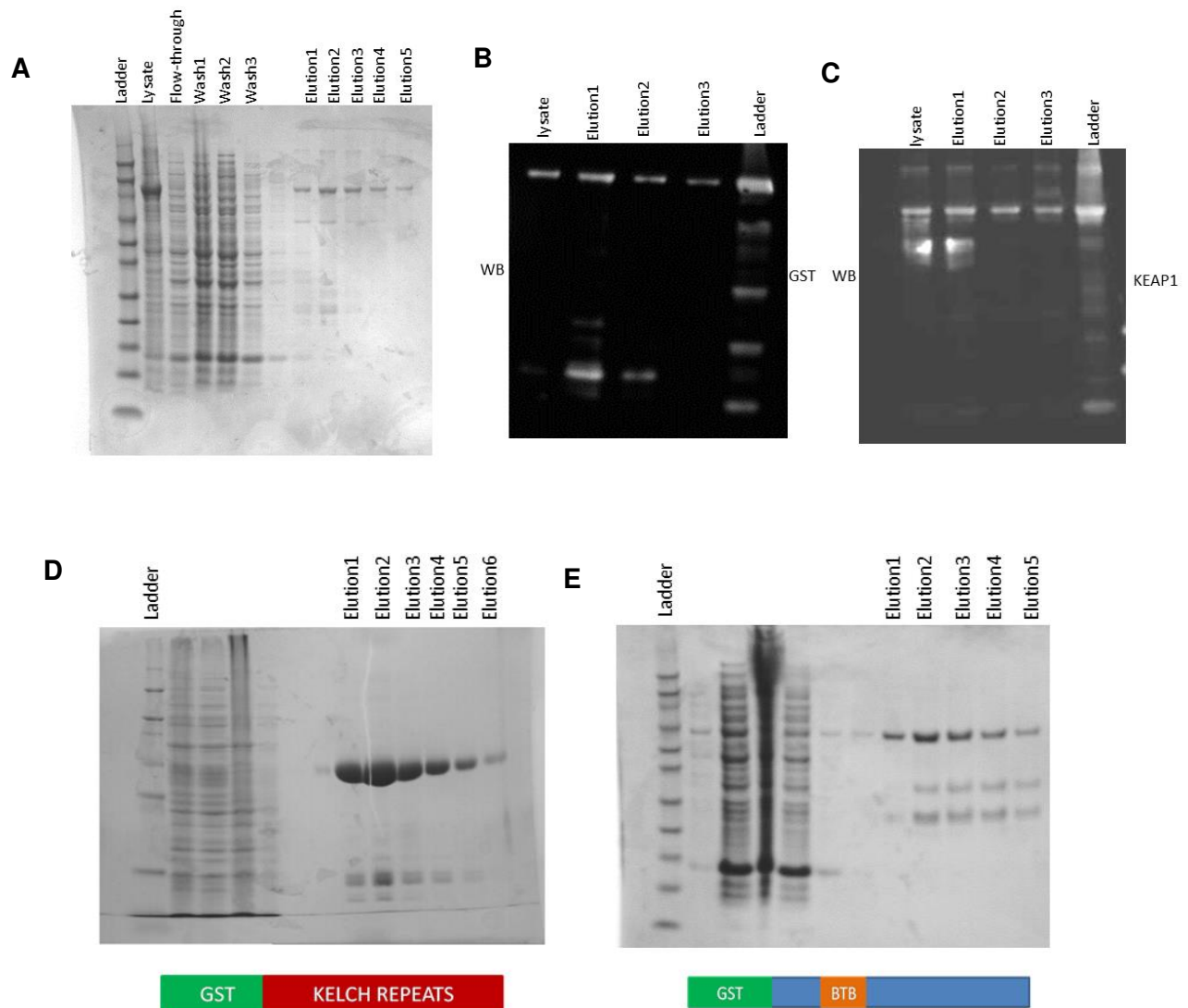


**Figure 4.4. Purification of GST tagged KEAP1, GST-KELCH, and GST-KEAP1 $\Delta$ KELCH.** (A) SDS-PAGE gel of the purification of full length GST-KEAP1 using GST affinity Chromatography. (B,C) Alternatively, samples from (A) have been analyzed by Western blot using antibodies against GST and KEAP1. (D) SDS-PAGE gel of the GST-KELCH repeats purification. (E) SDS-PAGE gel of GST-KEAP1 $\Delta$ KELCH purification.

### **4.3.3 FAM129B interacts directly with KEAP1 in vivo and in vitro.**

FAM129B has an ETGE motif at the carboxyl terminus, which potentially interacts with the KELCH like protein 1 (KEAP1). KEAP1 has also been shown to negatively regulate the NF-KB pathway[28]. So we aimed to see whether FAM129B and KEAP1 interact. Recombinant FAM129B with a GFP tag at the C-terminal and variable of deletion constructs were transfected into HEK293 cells as indicated in figure 4.5A. 24 hours post transfection, the cells were lysed and subjected to an Immuno-precipitation using antibodies against GFP. The samples were analyzed by western blotting using antibodies against FAM129B and KEAP1. The results show that FAM129B forms a complex with KEAP1. The ETGE motif of FAM129B is the site of interaction between of FAM129B and KEAP1, since FAM129B-ETAA-GFP , which has a mutated ETGE motif, disrupted the interaction (Figure 4.5B). Phosphorylation of the serine at residue 683 does not seem to have an effect on the interaction between FAM129B and KEAP1. FAM129B-S683D-GFP and FAM129B-S683A-GFP were both able to pull-down KEAP1 (Figure 4.5B). We then posed the question whether this interaction is direct. We performed a GST pull-down assay using purified recombinant KEAP1 with a GST tag and purified recombinant His-FAM129B. We also made deletion constructs of KEAP1: the KELCH domain by itself, and the full length KEAP1 without the KELCH domain. Both of these constructs were purified with a GST tag on their amino end and used in the GST pull-down assay with FAM129B. The resultant western blots showed that FAM129B and KEAP1 interact directly in vitro and that the KELCH domain is the site of interaction between KEAP1 and FAM129B. (Figure 4.6).

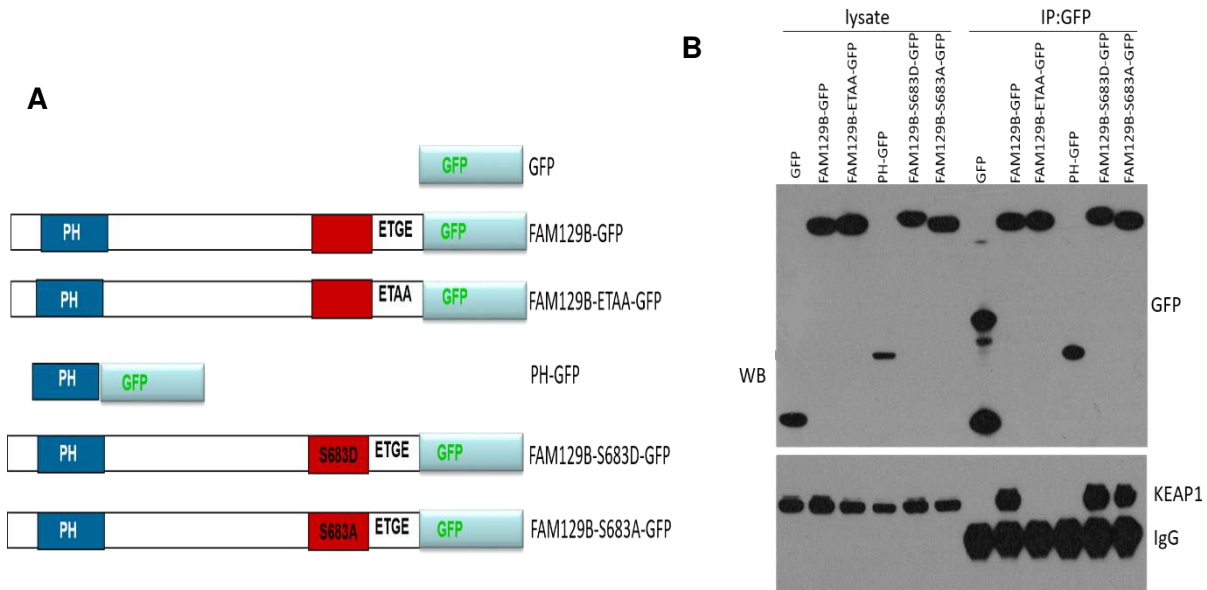


**Figure 4.5. FAM129B interacts with KEAP1 through its ETGE motif. (A)** Constructs used in the immunoprecipitation experiment in panel B. **(B)** HEK293 cells were transfected with the constructs in (A). 24 hours post-transfection, the cells were lysed and subjected to an immunoprecipitation using anti-GFP antibodies. The samples were then analyzed by an immuno-blot using antibodies against GFP and KEAP1. **(Song Chen, unpublished)**

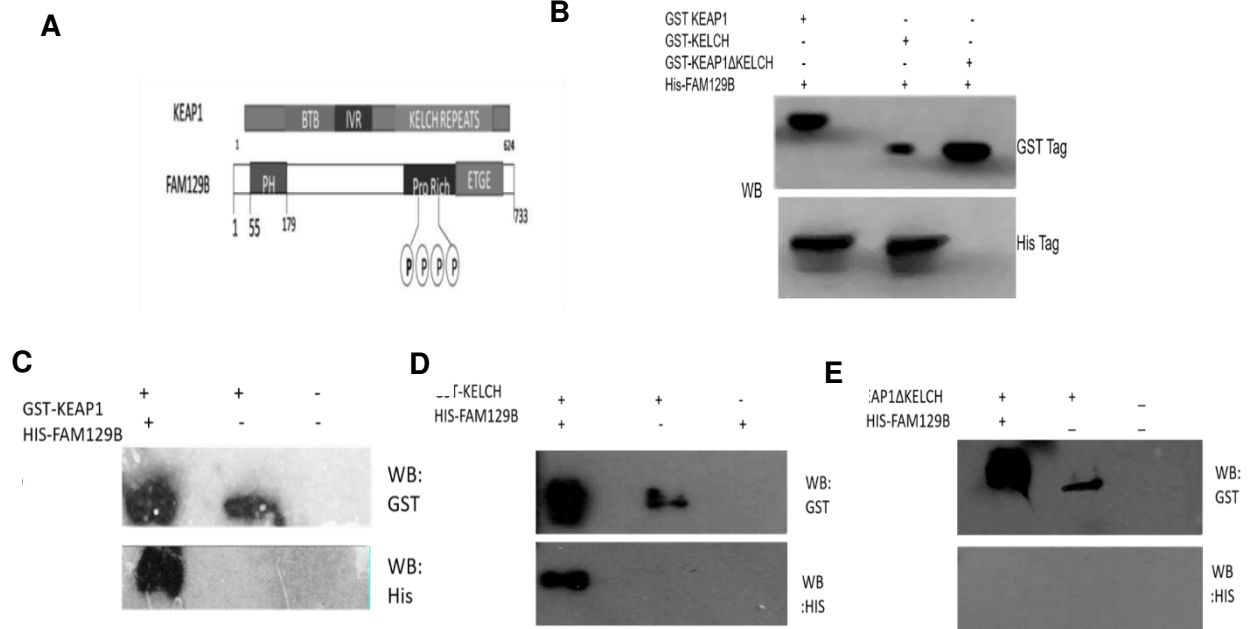


**Figure 4.6. FAM129B interacts with KEAP1 directly through the KECLH repeats of KEAP1. (A)** Domian structures of FAM129B and KEAP1. **(B,C,D,E)** . Purified GST-KEAP1, GST-KELCH, or GST-KEAP1ΔKELCH were incubated with GST resin to immobilize the GST tagged proteins. The resin was then washed and Recombinant His-FAM129B was added to the resin and incubated at 4°C with gentle shaking for 2 hours. The protein complexes were then eluted and analyzed by Western blot using GST antibodies and his-tag antibodies.

#### 4.3.4. Localization of FAM129B and KEAP1 upon TNF $\alpha$ treatment.

KEAP1 is primarily a cytosolic protein [31] while studies in our lab have shown that FAM129B is normally associated with the adherent junction. Since we hypothesize that FAM129B and KEAP1 interact to suppress TNF $\alpha$  induced apoptosis, we investigated the localization of FAM129B upon TNF $\alpha$  treatment. Indeed, immunofluorescent results show that FAM129B is mainly localized to the plasma membrane in the control where KEAP1 is dispersed throughout the cytoplasm. However, upon treating these HeLa cells with TNF $\alpha$  for 30 min, FAM129B is now no longer at the plasma membrane and is dispersed throughout the cytosol in a similar manner as KEAP1.

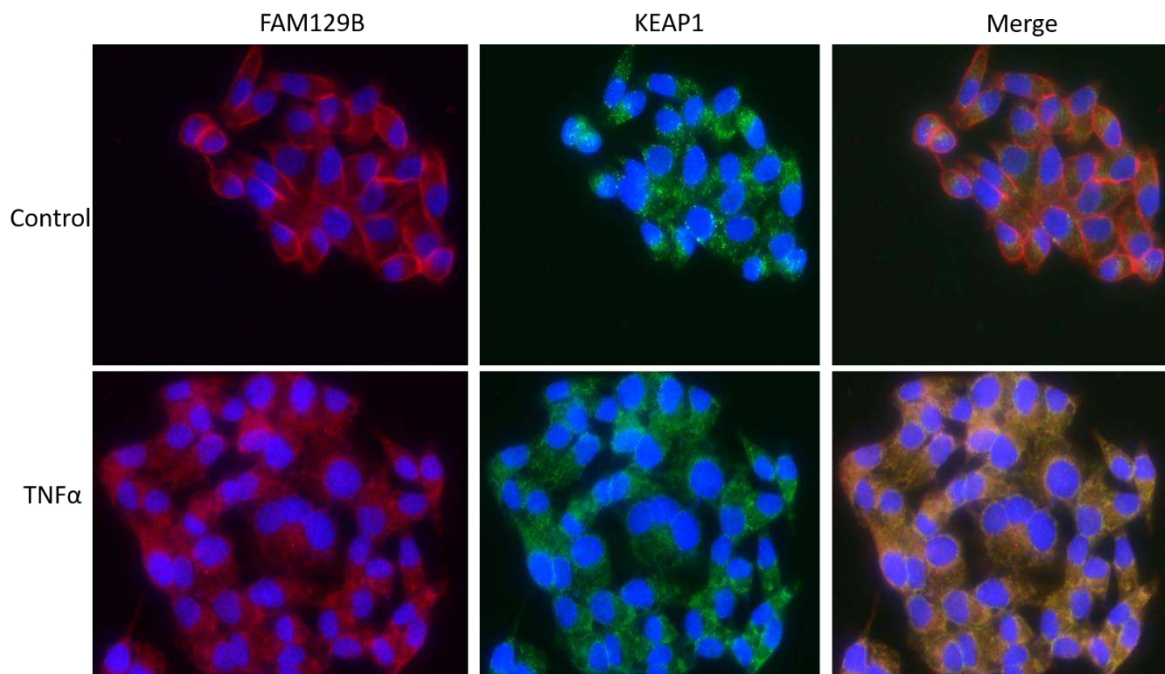


**Figure 4.7 FAM129B and KEAP1 seem to co-localize upon TNF $\alpha$  treatment in HeLa Cells.** HeLa cells grown on glass coverslips were incubated with TNF $\alpha$  (10 ng/ml) for 30 min. The cells were analyzed by Immunofluorescent Microscopy using antibodies FAM129B and KEAP1.



#### 4.4 Discussion

The transactivation of NF- $\kappa$ B is one of the many pathways regulated by KEAP1. KEAP1 has been shown to promote the TNF $\alpha$  apoptotic pathway by regulating IKK $\beta$  levels in the cell. IKK $\beta$ , binds to KEAP1 through its ETGE motif to KEAP1. Then KEAP1 binds to cul3 through its IVR domain. The cul3 protein then recruits the E3 Ubiquitin ligase and thus IKK $\beta$  gets targeted for proteasome degradation. This process, which prevents activation of NF- $\kappa$ B and the subsequent transcription of anti-apoptotic proteins, promotes [9, 28, 31, 32]. We showed that FAM129B and KEAP1 interact directly through the ETGE motif and the KELCH domain respectively by *ex-vivo* immunoprecipitations and *in-vitro* GST pull-down assays. It has been also reported that IKK $\beta$  binds to KEAP1 at the KELCH domain of KEAP1 [6], which implies that FAM129B and IKK $\beta$  may competitively bind to KEAP1. TNF $\alpha$  also might play a role in the interaction between FAM129B and KEAP1. Immunofluorescent results showed that FAM129B and KEAP1 co-localize in the cytosol upon TNF $\alpha$  treatment compared to the control where FAM129B is predominantly located at the adherent junction and KEAP1 is dispersed throughout the cytosol. This observation further supports the idea that interaction of KEAP1 and FAM129B is the reason why FAM129B suppresses the TNF $\alpha$  apoptotic pathway in HeLa cells. KEAP1 has been shown to promote apoptosis by targeting IKK $\beta$  for degradation [28]. When HeLa cells were treated with TNF $\alpha$ , FAM129B, which is normally localized at the membrane, moves to the cytosol where KEAP1 is present. FAM129B then interacts with KEAP1, thus disrupting the interaction between IKK $\beta$  and KEAP1. IKK $\beta$  is not targeted for degradation and activates the NF-

$\kappa$ B pathway and apoptosis is suppressed . However, further experiments need to be done to validate this conclusion

## CHAPTER 5

### THE ROLE OF FAM129B IN CANCER CELL INVASION

#### 5.1 Introduction

Suppression of apoptosis is a prerequisite for cancer cell invasion [12]. Preliminary data in our lab has shown that in exponentially growing HeLa cells, FAM129B was cytosolic but was translocated to the membrane when cells came in contact with each other[4] . Also knock-down of FAM129B expression reduced cancer cell movement through a matri-gel assay[22]. These findings suggest that FAM129B promotes cancer cell motility.

Metastasis is the process where cancer cells acquire genetic and biochemical changes, which allows the tumor cells to leave the primary tumor site and form colonies at a secondary site. Metastatic cells are the cause of 90% of cancer deaths[17]. Cancer cell invasion is a complex process where the biochemical and genetic make-up is still poorly understood.

Research into metastasis has revealed that adherent junction proteins are among the most altered proteins in metastatic cells. One of these proteins that is widely studied is E-Cadherin, a protein that is part of the classic cadherin family protein that mediate cell-cell interaction and helps organize the adherent junction. E-Cadherin forms a complex with  $\beta$ -catenin which is involved in regulating the cytoskeleton dynamics and modulating signal transduction pathways[33]. Forced expression of E-Cadherin in cultured cancer cells and a transgenic mice model impairs invasive and metastatic phenotypes whereas loss or interference in E-Cadherin function enhances both capabilities[12]. Thus, E-

cadherin acts as a suppressor of metastasis in epithelial cancers[12]. A process called the “Cadherin Switch” is a widely observed process in many metastatic or malignant cancers. Cadherin switching in cancers means the replacement of the E-Cadherin, which is an epithelial marker and a main component of the adherent junctions that keep the cells connected to one another, to N-Cadherin, which is a type of Cadherin that has a shorter extracellular region than E-cadherin and is regarded as a mesenchymal marker that promotes cell mobility. Invasive cell lines expression profiles show that N-Cadherin is highly expressed in these cell lines while E-Cadherin expression is negligible, an observation that supports the Cadherin Switching process[34, 35].

The epithelial to mesenchymal transition is a normal cellular process that is critical for morphogenesis and homeostasis of solid tissues. In cancer, EMT is highly upregulated. Malignant epithelial cells undergoing EMT acquire properties that facilitate metastatic spread. EMT also renders cancer cells resistant to different types of therapies, often by reducing apoptotic sensitivity [18]. Also, metastatic cancer cell lines have elevated expression of mesenchymal markers such as vimentin and negligible expression of epithelial markers such as E-Cadherin[36]. EMT is induced by chemokines such as Transforming Growth Factor Beta (TGF $\beta$ )[37]. The adherent junctions that connect the cells to one other degrade as proteins that are associated with epithelial morphology, such as E-Cadherin, occludens, and claudins are degraded. At the same time, proteins responsible for mesenchymal morphology, such as N-Cadherin, SNAIL, and vimentin are upregulated. Matrix Metalloproteinases (MMPs) are also upregulated and degrade the basement membrane and extracellular matrix (ECM) to promote the detachment of the mesenchymal cells[38].

In this chapter, we reveal that FAM129B expression is upregulated by the epithelial to mesenchymal transition. We also show that FAM129B phosphorylation by MAP kinase translocates the protein to membrane while inhibiting MAP kinase removes FAM129B from the membrane. These findings confirm the role of FAM129B in cancer cell invasion.

## **5.2 Materials and Methods**

### **5.2.1 Antibodies and Reagents:**

Antibodies directed against FAM129B , N-cadherin, and Vimentin were purchased from Cell signaling Technology. GAPDH antibodies and N-cadherin siRNA were from Santa Cruz Biotechnology. TGF $\beta$  was purchased from Genscript. EGF , U1206 , and PD10356 were from Sigma.

### **5.2.3 MAPK Kinase Pathway Activation:**

HeLa cells incubated in serum-free DMEM media for 18-20 hours were treated with EGF (10 nM) or PMA (10  $\mu$ M) for 30 minutes. FAM129B localization was then analyzed by immuno-fluorescence microscopy. Alternatively, cells treated with EGF and PMA for 30 minutes were then treated with specific MEK inhibitors U1026(10  $\mu$ M) and PD10356 (10  $\mu$ M) for an hour prior to FAM129B localization analysis.

### **5.2.4 Epithelial to Mesenchymal transition (EMT) induction.**

A549 cells growing in RPMI media were first serum-starved for 18-20 hours. EMT was induced by TGF $\beta$  (10 ng/ml) treatment for 48 hours,. The cells were then lysed and the

lysate was analyzed by Immuno-blotting using antibodies for FAM129B, GAPDH (loading control ) and vimentin (mesenchymal marker) to check for transition success.

### **5.2.5 Immuno-fluorescence Microscopy:**

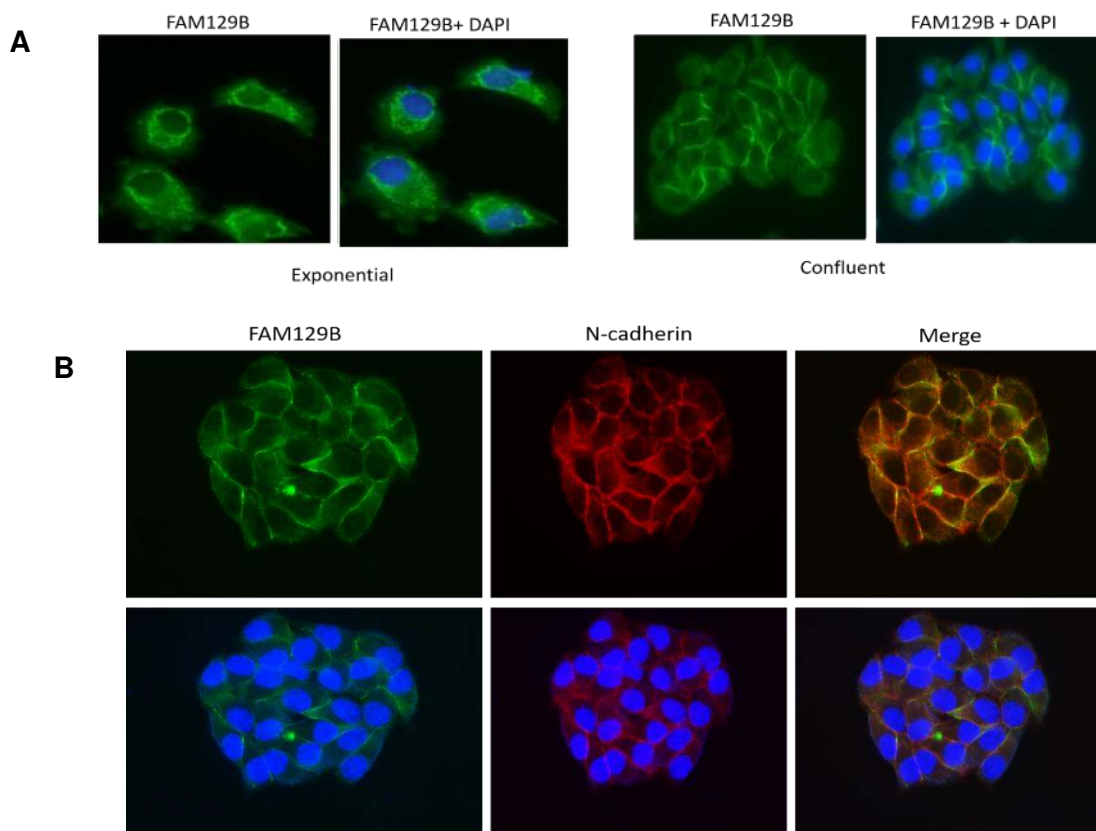
HeLa cells were seeded on cover slips in a 6-well plate and serum starved overnight. The cells were washed three times with PBS, fixated with 10% formalin, and permeabilized with 0.2% Triton-X. After blocking with 1% BSA in PBS for 1 hour, the cells were washed 3X with PBS and then incubated with either FAM129B rabbit with or without either N-cadherin antibodies (1:100 dilution) for 2 hours. The cover-slips were washed with PBS and incubated for 1 hour with either Alexa flour 488 Goat anti-Rabbit and 594 Goat anti-mouse. After washing with PBS, the coverslips were then mounted on microscope slides using Prolong Gold Anti-Fade mountant with DAPI (Life technologies, P36931). The microscope slides were then dried in the dark at 4°C overnight. The cells were then visualized using a Nikon E8000 fluorescent microscope.

## **5.3 Results**

### **5.3.1 Immunofluorescent data show that FAM129B localizes to the adherent junctions where it co-localizes with N-Cadherin**

Preliminary data in our lab has shown that FAM129B localizes at the cell membrane when cells are in contact with each other. We wanted to check whether FAM129B is associated with any of the adherent junction proteins such N-cadherin. To test this, co-localization experiments between FAM129B and N-cadherin using immunofluorescence

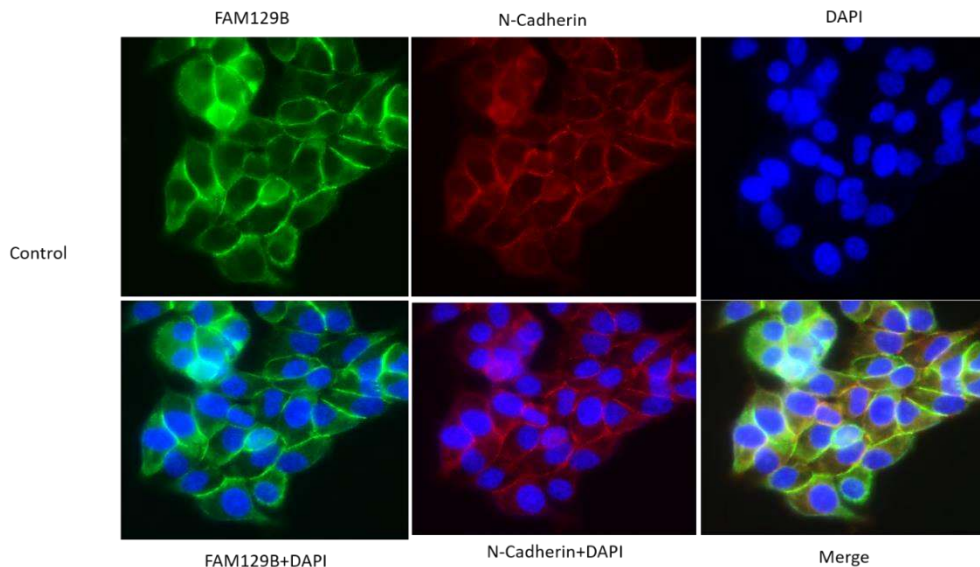
were conducted. The results showed that FAM129B localizes to the membrane in confluent HeLa cells while it is dispersed throughout the cytosol in non-confluent cells(Figure 5.1A). Figure 5.1 B shows that N-cadherin is also at the membrane in confluent cells indicating that FAM129B and N-cadherin co-localize at the membrane in confluent HeLa cells.



**Figure 5.1. FAM129B co-localizes with N-Cadherin in Confluent HeLa cells. (A)** Immunofluorescent images of endogenous FAM129B (green) in exponentially growing HeLa cells and in confluent HeLa cells. **(B)** HeLa cells grown on glass cover slips were stained for FAM129B (green) and N-Cadherin (red). Images were taken using a Nikon E800 fluorescent microscope

### 5.3.2 Knockdown of N-cadherin expression displaces FAM129B from the membrane in confluent HeLa cells.

Since FAM129B co-localizes with N-cadherin in HeLa cells, we decided to test whether N-cadherin knockdown has any effect on FAM129B localization. To test this hypothesis, N-cadherin expression was knocked-down using siRNA technology and cells were analyzed using Immuno-fluorescent microscopy. The results show that in the control cells, FAM129B and N-cadherin co-localize at the membrane. However, in the transfected cells, N-cadherin expression is completely knocked down and that FAM129B is dispersed throughout the cytoplasm in these cells.(Figure 5.2).





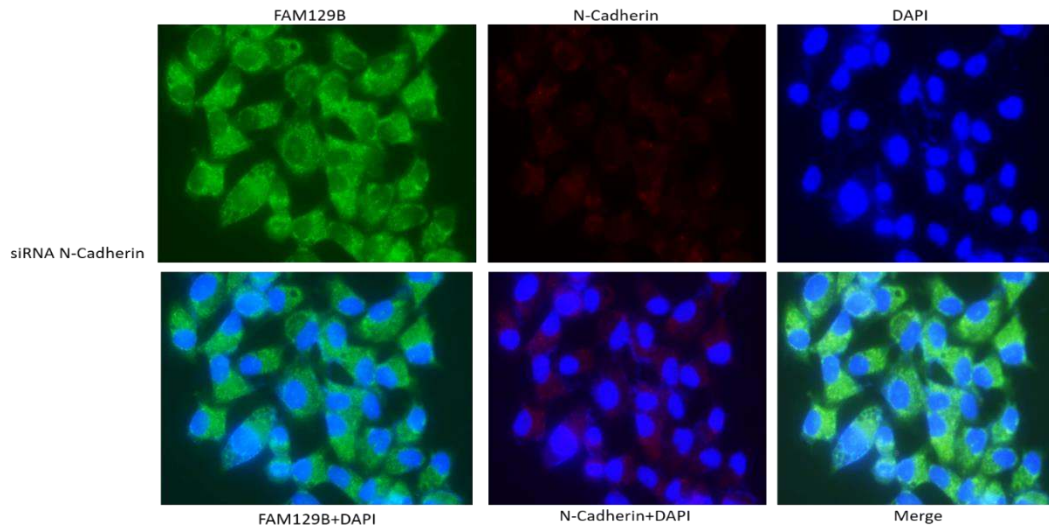


**Figure 5.2. Knockdown of N-Cadherin expression in HeLa seems to inhibit FAM129B localization to the membrane.** HeLa cells grown on glass cover slips were transfected with siRNA N-cadherin. 48 hr post transfection, the cells were analyzed by Immunofluorescent microscopy using antibodies against FAM129B (green) and N-Cadherin (red).

### 5.3.2 MAP Kinase phosphorylation of FAM129B localizes FAM129B to the plasma membrane

Old et al has reported that FAM129B is localized to the plasma membrane in melanoma cells upon treatment with MAP kinase inhibitors[3]. We decided to investigate whether phosphorylation of FAM129B has any effect on localization of FAM129B in confluent HeLa cells. Immunofluorescent results showed that contrary to the literature, FAM129B was localized to the membrane upon treatment with EGF which activates MAP kinase. Thus, phosphorylation of FAM129B localizes FAM129B to the membrane while treatment with two different MEK inhibitors, PD98059 and U1026, removes FAM129B completely from the membrane.

FAM129B was also localized to the membrane in PMA treated cells where MAP Kinase is indirectly activated while treatment of these cells with MEK inhibitor U1026 translocated FAM129B back to the cytosol. (Figure 5.4)

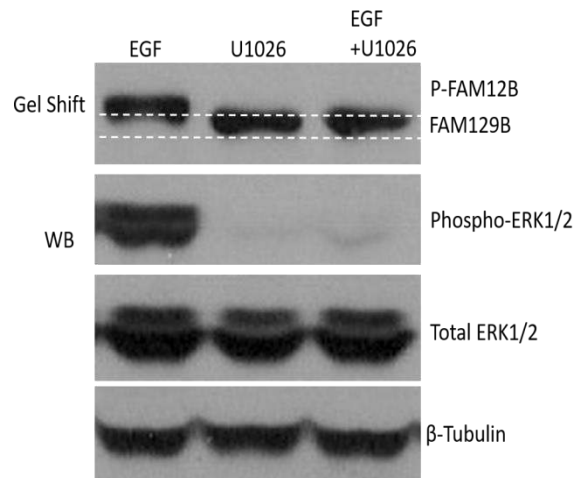


**Figure 5.3. FAM129B is phosphorylated by MAP Kinase.** HeLa cells were treated with with EGF, U1026, or EGF and U1026. The cells were then lysed and analyzed by Western blot. The shift in the FAM129B indicates phosphorylation of FAM129B by MAP Kinase. **(Song Chen, unpublished )**

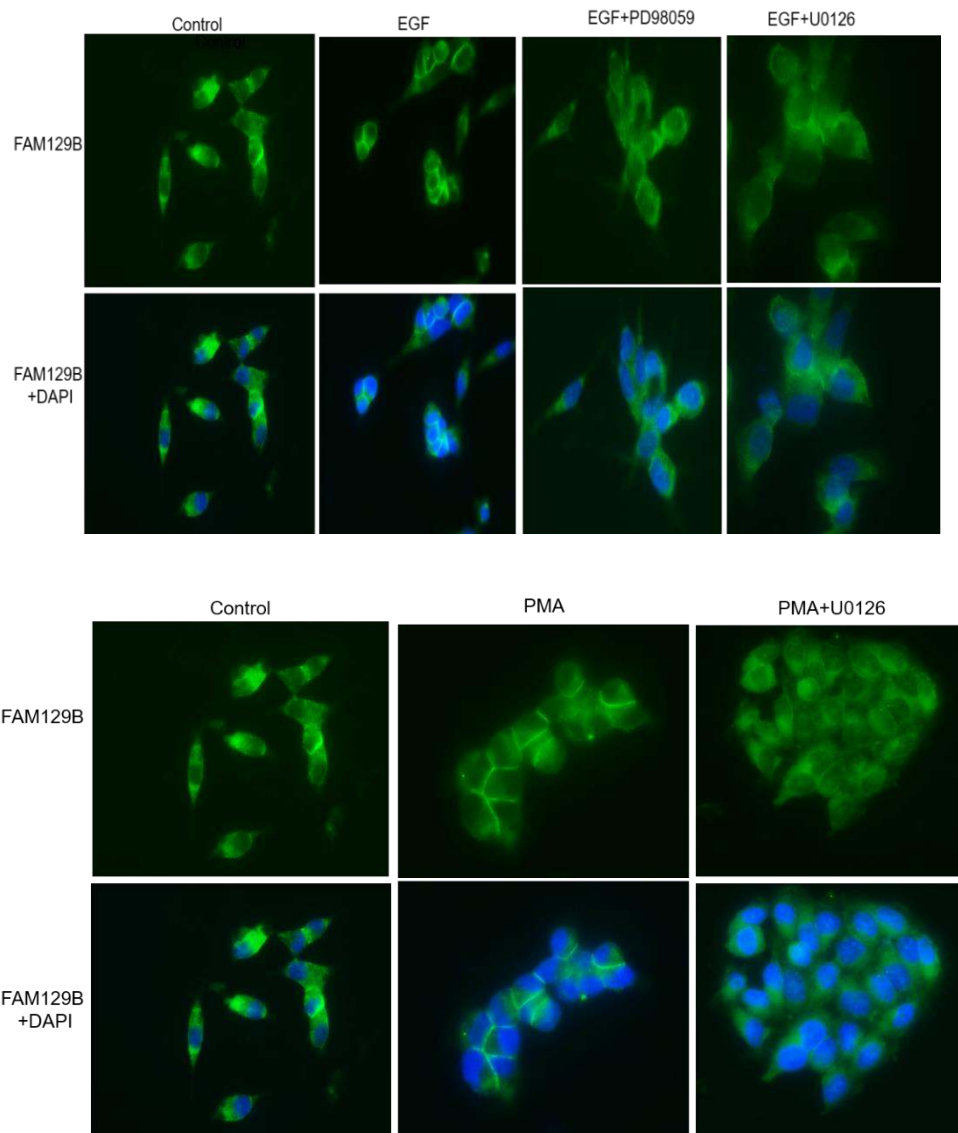


**Figure 5.4. FAM129B phosphorylation by MAP kinase translocate FAM129B to the membrane.** HeLa cells grown on glass cover slips were treated with different activators and inhibitors indicated in the figure. The cells were then fixed and analyzed by immunofluorescent microscopy.

### 5.3.3 FAM129B expression is upregulated when EMT is induced in A549 cells

FAM129B is expressed at high levels in cell lines when vimentin was upregulated[22]. Vimentin is a mesenchymal marker[38] so we wanted to see whether Epithelial to Mesenchymal transition affects FAM129B expression. Treatment of A549 cells with TGF $\beta$ 1 for 48 hours shows that EMT was induced successfully since vimentin was expressed. The resulting western blot also showed that FAM129B expression increased upon EMT induction in A549 cells (Figure 5.5).

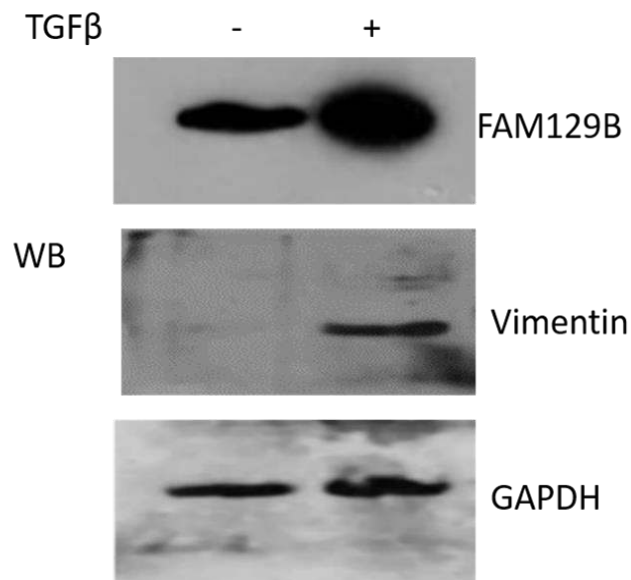


**Figure 5.5. FAM129B expression level increases when EMT is induced by TGF $\beta$ .** A549 cells (lung cancer cells) were grown in 60 mm dish in RPMI and 10% FBS. When the cells were 80% confluent, the media was replaced with 1% RPMI medium and EMT was induced with TGF $\beta$  (20 ng) for 48 hours. The cells were then lysed and analyzed by western blotting. Vimentin was used as mesenchymal marker. GAPDH was used as a loading control.

## 5.4 Discussion

FAM129B was first identified in the literature as an adherent junction associated protein[4]. Results in our lab have consistently shown that FAM129B might be involved in cancer cell invasion. FAM129B is highly expressed in metastatic cell lines compared to non-invasive cell lines. Furthermore, knockdown of FAM129B in invasive breast cancer cell line MDA-MB-231 decreased cancer cell motility *in vitro* [22].

Consistent with previous findings, FAM129B is localized to the cell membrane when HeLa cells are in contact with each other. This led to the hypothesis that FAM129B might interact with adherent junction proteins at the membrane. Co-localization experiments showed that FAM129B is localized at the adherent junction with N-cadherin. FAM129B is displaced from the cell membrane when N-cadherin expression is knocked-down as a result of disruption of the junction. These results confirm that FAM129B is associated with the adherent junction. Another possibility is that FAM129B interacts with phospholipids at the membrane via its Pleckstrin homology (PH domain), which has yet to be investigated. The association of FAM129B with the membrane suggests that the protein could be involved in various cellular signaling cascades or might play the role in regulating the adherent junction dynamics, which is another possible mechanism for the role of FAM129B in cancer cell invasion

As mentioned several times previously, FAM129B has several phosphorylation sites at its carboxyl-terminus. Old et al also mentioned in his study that

phosphorylation of FAM129B promoted melanoma cell invasion *in vitro* and also affected FAM129B localization to the membrane. We decided to test this result in HeLa cells. Activation of MAP kinase by both EGF and PMA has caused FAM129B to localize to the membrane in HeLa cells. While treatment with MEK inhibitors for both the EGF and PMA treated cells re-located FAM129B into the cytosol, indicating that in both treatments, the localization effect is specifically due to MAP kinase. MAP kinase activation has been reported to be associated with cellular migration. Treatment of cells with EGF and TGF $\beta$  together also promotes the epithelial to mesenchymal (EMT) activation at a faster rate than TGF $\beta$  alone in cell culture [39]. Therefore, FAM129B phosphorylation could play a major role in cancer cell invasion by accelerating EMT induction.

The epithelial to mesenchymal transition is a process where cells undergo biochemical and morphological changes that enables cells to move from one place to another. EMT is a naturally occurring process during development and wound healing and is tightly regulated. In cancer cells, several studies have reported that EMT is upregulated in cancer cells and helps tumors acquire metastatic properties[36]. FAM129B is upregulated in cell lines where vimentin was expressed[22] so we investigated if FAM129B might be essential for EMT. Induction of EMT in A549 cells, a cell line that is widely used for EMT studies[40], increased FAM129B compared to controls. This finding shows that FAM129B expression is induced by TGF $\beta$  and that FAM129B may play a role in the epithelial to mesenchymal transition. My hypothesis is that FAM129B promotes cancer cell

mobility through its association with the adherent junction. Still, further experiments need to be done to validate this hypothesis.

**REFERENCES**

1. Yuki, R., et al., *Overexpression of zinc-finger protein 777 (ZNF777) inhibits proliferation at low cell density through down-regulation of FAM129A*. J Cell Biochem, 2015. **116**(6): p. 954-68.
2. Boyd, R.S., et al., *Proteomic analysis of the cell-surface membrane in chronic lymphocytic leukemia: identification of two novel proteins, BCNP1 and MIG2B*. Leukemia, 2003. **17**(8): p. 1605-12.
3. Old, W.M., et al., *Functional proteomics identifies targets of phosphorylation by B-Raf signaling in melanoma*. Mol Cell, 2009. **34**(1): p. 115-31.
4. Chen, S., H.G. Evans, and D.R. Evans, *FAM129B/MINERVA, a novel adherens junction-associated protein, suppresses apoptosis in HeLa cells*. J Biol Chem, 2011. **286**(12): p. 10201-9.
5. Oishi, H., et al., *Delayed cutaneous wound healing in Fam129b/Minerva-deficient mice*. J Biochem, 2012. **152**(6): p. 549-55.
6. Conrad, W., et al., *FAM129B is a novel regulator of Wnt/beta-catenin signal transduction in melanoma cells*. F1000Res, 2013. **2**: p. 134.
7. Ji, H., et al., *EGFR phosphorylates FAM129B to promote Ras activation*. Proc Natl Acad Sci U S A, 2016. **113**(3): p. 644-9.
8. Lemmon, M.A., *Pleckstrin homology (PH) domains and phosphoinositides*. Biochem Soc Symp, 2007(74): p. 81-93.
9. Tian, H., et al., *Keap1: one stone kills three birds Nrf2, IKKbeta and Bcl-2/Bcl-xL*. Cancer Lett, 2012. **325**(1): p. 26-34.



10. Lin, Y., et al., *The NF-kappaB activation pathways, emerging molecular targets for cancer prevention and therapy*. Expert Opin Ther Targets, 2010. **14**(1): p. 45-55.
11. Su, Z., et al., *Apoptosis, autophagy, necroptosis, and cancer metastasis*. Mol Cancer, 2015. **14**: p. 48.
12. Hanahan, D. and R.A. Weinberg, *Hallmarks of cancer: the next generation*. Cell, 2011. **144**(5): p. 646-74.
13. Elmore, S., *Apoptosis: a review of programmed cell death*. Toxicol Pathol, 2007. **35**(4): p. 495-516.
14. Wang, C. and R.J. Youle, *The role of mitochondria in apoptosis\**. Annu Rev Genet, 2009. **43**: p. 95-118.
15. Kruidering, M. and G.I. Evan, *Caspase-8 in apoptosis: the beginning of "the end"?* IUBMB Life, 2000. **50**(2): p. 85-90.
16. Park, Y.H., et al., *Simvastatin induces apoptosis in castrate resistant prostate cancer cells by deregulating nuclear factor-kappaB pathway*. J Urol, 2013. **189**(4): p. 1547-52.
17. Jemal, A., et al., *Cancer statistics, 2010*. CA Cancer J Clin, 2010. **60**(5): p. 277-300.
18. Lu, M., et al., *E-cadherin couples death receptors to the cytoskeleton to regulate apoptosis*. Mol Cell, 2014. **54**(6): p. 987-98.
19. Massague, J. and A.C. Obenauf, *Metastatic colonization by circulating tumour cells*. Nature, 2016. **529**(7586): p. 298-306.

20. Nicolson, G.L., *Cancer metastasis: tumor cell and host organ properties important in metastasis to specific secondary sites*. Biochim Biophys Acta, 1988. **948**(2): p. 175-224.
21. Principe, D.R., et al., *TGF-beta: duality of function between tumor prevention and carcinogenesis*. J Natl Cancer Inst, 2014. **106**(2): p. djt369.
22. Chen, S., *The role of CAD, FLASH and FAM129B in cancer cell survival and apoptosis*. 2012. p. 186 p.
23. Luft, J.R., J. Newman, and E.H. Snell, *Crystallization screening: the influence of history on current practice*. Acta Crystallogr F Struct Biol Commun, 2014. **70**(Pt 7): p. 835-53.
24. Dobson, C.M., *Principles of protein folding, misfolding and aggregation*. Semin Cell Dev Biol, 2004. **15**(1): p. 3-16.
25. Whitmore, L., et al., *DichroMatch at the Protein Circular Dichroism Data Bank (DM@PCDDDB): A Web-based Tool for Identifying Protein Nearest Neighbors using Circular Dichroism Spectroscopy*. Protein Sci, 2017.
26. Walden, H., *Selenium incorporation using recombinant techniques*. Acta Crystallogr D Biol Crystallogr, 2010. **66**(Pt 4): p. 352-7.
27. Li, X., et al., *Crystal structure of the Kelch domain of human Keap1*. J Biol Chem, 2004. **279**(52): p. 54750-8.
28. Lee, D.F., et al., *KEAP1 E3 ligase-mediated downregulation of NF-kappaB signaling by targeting IKKbeta*. Mol Cell, 2009. **36**(1): p. 131-40.

29. Camp, N.D., et al., *Wilms tumor gene on X chromosome (WTX) inhibits degradation of NRF2 protein through competitive binding to KEAP1 protein*. J Biol Chem, 2012. **287**(9): p. 6539-50.
30. Greten, F.R., et al., *IKKbeta links inflammation and tumorigenesis in a mouse model of colitis-associated cancer*. Cell, 2004. **118**(3): p. 285-96.
31. Kim, J.E., et al., *Suppression of NF-kappaB signaling by KEAP1 regulation of IKKbeta activity through autophagic degradation and inhibition of phosphorylation*. Cell Signal, 2010. **22**(11): p. 1645-54.
32. Thu, K.L., et al., *Genetic disruption of KEAP1/CUL3 E3 ubiquitin ligase complex components is a key mechanism of NF-kappaB pathway activation in lung cancer*. J Thorac Oncol, 2011. **6**(9): p. 1521-9.
33. Hartsock, A. and W.J. Nelson, *Adherens and tight junctions: structure, function and connections to the actin cytoskeleton*. Biochim Biophys Acta, 2008. **1778**(3): p. 660-9.
34. Gil, D., et al., *Integrin-linked kinase regulates cadherin switch in bladder cancer*. Tumour Biol, 2016. **37**(11): p. 15185-15191.
35. Gheldof, A. and G. Berx, *Cadherins and epithelial-to-mesenchymal transition*. Prog Mol Biol Transl Sci, 2013. **116**: p. 317-36.
36. Suarez-Carmona, M., et al., *EMT and inflammation: inseparable actors of cancer progression*. Mol Oncol, 2017.
37. Rasanen, K. and A. Vaheri, *TGF-beta1 causes epithelial-mesenchymal transition in HaCaT derivatives, but induces expression of COX-2 and migration only in benign, not in malignant keratinocytes*. J Dermatol Sci, 2010. **58**(2): p. 97-104.

38. Prieto-Garcia, E., et al., *Epithelial-to-mesenchymal transition in tumor progression*. Med Oncol, 2017. **34**(7): p. 122.
39. Uttamsingh, S., et al., *Synergistic effect between EGF and TGF-beta1 in inducing oncogenic properties of intestinal epithelial cells*. Oncogene, 2008. **27**(18): p. 2626-34.
40. Tan, W.J., et al., *Calpain 1 regulates TGF-beta1-induced epithelial-mesenchymal transition in human lung epithelial cells via PI3K/Akt signaling pathway*. Am J Transl Res, 2017. **9**(3): p. 1402-1409.

**ABSTRACT****FAM129B , A NOVEL ADHERENT JUNCTION PROTEIN, FORMS A COMPLEX WITH KEAP1**

by

**FATME HACHEM**

July 2017

Advisor: Dr. David Evans

Major: Biochemistry and Molecular Biology

Degree: Master of Science

FAM129B/Minerva, a protein implicated in melanoma cell invasion, has been shown to suppress TNF $\alpha$  induced apoptosis in cancer cells (Song, Evans & Evans (2010), JBC 286, 10201-09), thus contributing to the survival of metastatic cells. KEAP1, a substrate recognition molecule for the CUL3 E3 ubiquitin ligase, plays a central role in the activation of the TNF $\alpha$  pathway. We wish to test the hypothesis that the up-regulation of FAM129B in cancer cells suppresses apoptosis by sequestering KEAP1, thus preventing its participation in the apoptotic pathway. The first step is to demonstrate that FAM129B and KEAP1 form a complex. We have cloned and expressed the proteins in *E. coli* and purified both to homogeneity. Pull downs and immunoprecipitation clearly showed that the two proteins form a high affinity, stoichiometric complex. Using individually cloned domains, as well as mutations of the ETGE motif in FAM129B, the binding sites on each protein have been located. The proline rich region of FAM129B was shown elsewhere (Old et. al. (2009) Mol Cell.34,115) to be phosphorylated by MAP

kinase (Erk1/2) at four sites. The effect of MAP kinase, which is upregulated in cancer cells, and PKC phosphorylation on the stability and formation of the complex has also been investigated.

**AUTOBIOGRAPHICAL STATEMENT****FATME HACHEM****Education:**

2017 MS. Major: Biochemistry and Molecular Biology

Wayne State University School of Medicine, Detroit, MI USA

2011 B.S. Major: Biochemistry

University of Michigan-Dearborn

**Publications:**

- Evans HG, Fernando R, Vaishnav A, Kotichukkala M, Heyl D, **Hachem F**, Brunzelle JS, Edwards BF , Evans DR, “ *Intersubunit Communication in the Dihydroorotase-Aspartate Transcarbamoylase complex of Aquifex Aeolicus*” , Protein Science, 2014 Jan , vol 23 p 100-109 , PMID : 24553170
- Hervé G, Evans HG, Fernando R, Patel C, **Hachem F**, Evans DR.” *Activation of latent dihydroorotase from Aquifex aeolicus by pressure*”, J Biol Chem. 2016 Oct 16. pii: jbc.M116.739862, PMID:27746403